Supporting Information

Arginine-linked neomycin B dimers: synthesis, rRNA binding, and resistance enzyme activity

Yi Jin,[a] Derrick Watkins,[b] Natalya N. Degtyareva,[b] Keith D. Green,[c] Meredith N. Spano,[b] Sylvie Garneau-Tsodikova,[c,*] and Dev P. Arya,[a,b,*]

[a] Department of Chemistry, Clemson University, Clemson, SC 29634, USA. [b] NUBAD, LLC., Greenville, SC 29605, USA. [c] Department of Pharmaceutical Sciences, University of Kentucky, Lexington, KY, 40536-0596, USA.

Table of contents Page #

Abbreviations: NMP, 1-methyl-2-pyrrolidinone; TIPS, triisopropylsilane; TPSCl, 2,4,6-triisopropyl benzenesulfonylchloride.

Materials and instrumentation. Unless otherwise specified, chemicals were purchased from commercially available sources and used without further purification. The *E. coli* A-site (5'-GGCGUCACACCUUCGGGUAAGUCGCC-3') and human A-site (5'-GGCGUCGCUACUUCGGUAAAAGUCGCC-3') models with a 2' ACE protecting group were purchased from Thermo Scientific Dharmacon. RNA oligomers were deprotected according to the manufacturer's protocol, and the deprotection buffer was removed by evaporation using SpeedVac (GeneVac). All oligomers were resuspended in buffer prepared in DEPC-treated H_2O (OmniPure) and their concentrations were determined by NanoQuant Plate (Infinite M1000 Pro, Tecan) using absorption coefficients at 260 nm provided by the manufacturer. Neomycin B (NEO, Fisher), F-NEO, and compounds **6-16** were dissolved in DEPC-treated H_2O (OmniPure or Fisher) to desired concentrations. F-NEO was synthesized and purified as described before.[1] F-NEO concentration was checked by absorbance at 485 nm ($\varepsilon_{485\ nm}$ = 13,260 $M^{-1}cm^{-1}$). ^1H and ^{13}C NMR spectra were recorded on a JEOL (Tokyo, Japan) ECA 500 MHz FT-NMR spectrometer,

Bruker Avance-300 spectrometer, or Bruker Avance-500 spectrometer. Mass spectra (MALDI-TOF) were recorded using a Bruker Daltonics/Omniflex MALDI-TOF spectrometer.

Chemistry:

Experimental procedures for the preparation of compounds 2-15 and their characterization (Fig. S1)**.**

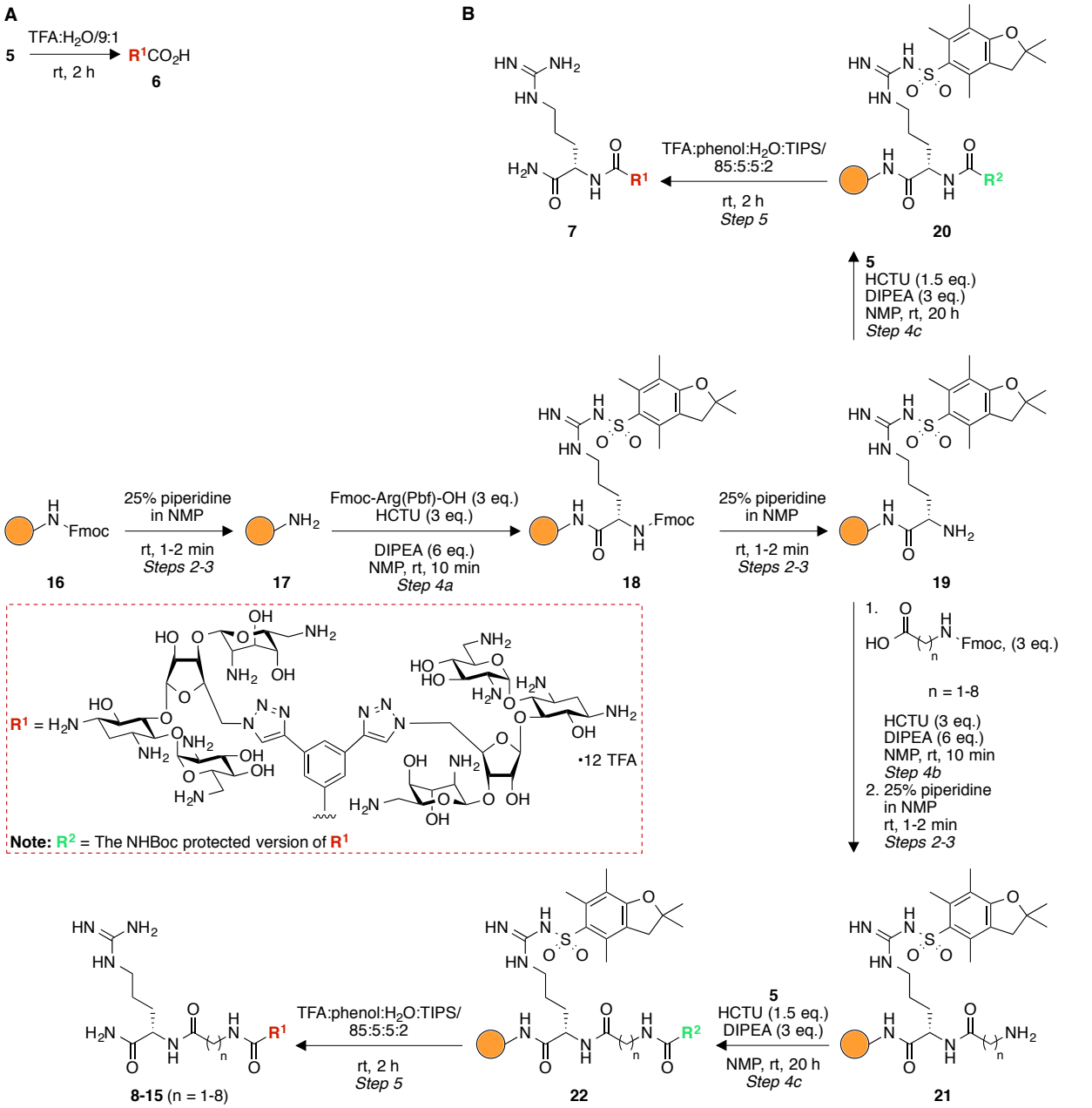

Fig. S1. Solid-phase synthesis of **A.** a control molecule, NEO dimer acid (**6**), and **B.** L-arginine NEO dimer conjugates **7-15**.

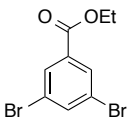

Preparation of ethyl 3,5-dibromobenzoate (2). The known compound **2** was synthesized following a previously published procedure with slight modifications (Fig. 1).[2] 98% sulfuric acid (1.0 mL) was added to a suspension of 3,5-

dibromobenzoic acid (**1**) (5.60 g, 20 mmol) in EtOH (20 mL). The reaction mixture was refluxed for 22 h. 10 mL of the solvent was then removed under normal pressure and the reaction mixture was poured into ice-H_2O. The resulting precipitate was filtered and washed with a saturated $NaHCO_3$ solution and H_2O to give the desired ethyl 3,5-dibromobenzoate (**2**) (5.40 g, 88%) as a white solid: ^{1}H NMR (500 MHz, $(CD_3)_2SO$) δ 8.16 (t, J = 1.8 Hz, 1H), 8.03 (d, J = 1.8 Hz, 2H), 4.33 (q, J = 7.1 Hz, 2H), 1.33 (t, J = 7.1 Hz, 3H); ^{13}C NMR (125 MHz, $(CD_3)_2SO$) δ 163.68, 138.36, 134.02, 131.22, 123.30, 62.19, 14.45.

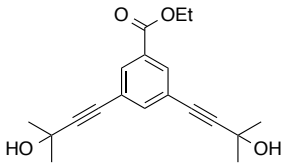

Preparation of ethyl 3,5-bis(3-hydroxy-3-methylbut-1-yn-1-yl)benzoate (3). The known compound **3** was synthesized following a previously published procedure with slight modifications (Fig. 1).[2, 3] A mixture of ethyl 3,5-dibromobenzoate (**2**) (0.15 g, 0.50 mmol), 2-methylbut-3-yn-2-ol (0.13 g, 1.5 mmol), THF (3.0 mL), and Et_3N (3.0 mL) was stirred under Ar for 30 min. $Pd(PPh_3)_2Cl_2$ (17 mg, 0.025 mmol) and CuI (9.5 mg, 0.05 mmol) were then added to the solution. The reaction mixture was stirred for 15 h at 80 °C. The solvent was removed under reduced pressure. The residual solid was washed with H_2O and purified by column chromatography (SiO_2, CH_2Cl_2:EtOAc/5:1) to afford the desired compound **3** (149 mg, 95%) as a brown oil: ^{1}H NMR (500 MHz, $(CD_3)_2SO$) δ 7.84 (d, J = 1.6 Hz, 2H), 7.61 (t, J = 1.6 Hz, 1H), 5.55 (s, 2H), 4.33 (q, J = 7.1 Hz, 2H), 1.48 (s, 12H), 1.34 (t, J = 7.1 Hz, 3H).

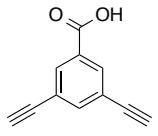

Preparation of 3,5-Diethynylbenzoic acid (4). The known compound **4** was synthesized following a previously published procedure with slight modifications (Fig. 1).[2, 3] A mixture of ethyl 3,5-bis(3-hydroxy-3-methylbut-1-yn-1-yl)benzoate (**3**) (0.31 g, 1.0 mmol), KOH (0.34 g, 6.0 mmol), and *i*-PrOH (5.0 mL) was stirred for 4 h at 90 °C. After cooling to room temperature, the reaction mixture was acidified to pH 2 by using 1 M HCl, and then was extracted trice with EtOAc. The EtOAc layer was washed with H_2O. The solvent was then removed and the residual solid was purified by column chromatography (SiO_2, CH_2Cl_2:EtOAc:AcOH/250:50:1) to afford the desired compound **4** (100 mg, 59%) as white solid: ^{1}H NMR (500 MHz, $CDCl_3$) δ 8.21 (d, J = 1.5 Hz, 2H), 7.85 (t, J = 1.5 Hz, 1H), 3.19 (s, 2H).

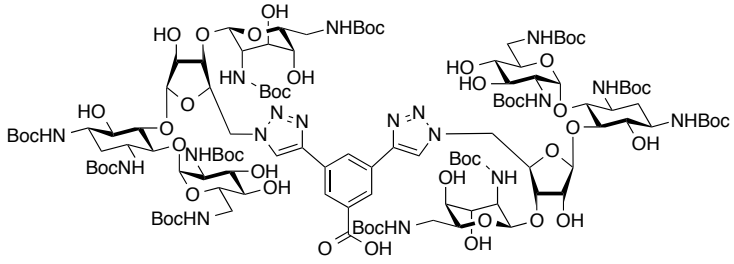

Preparation of Boc-protected NEO dimer (5). A mixture of NEO sulfate (9.09 g, 10.0 mmol), Na_2CO_3 (13.78 g, 130.0 mmol), di-*tert*-butyl dicarbonate (28.37 g, 130.0 mmol), H_2O (480 mL), and MeOH (480 mL) was stirred at room temperature for 3 h. After removal of 500 mL of the solvent under reduced pressure, the solid was collected by filtration and washed with H_2O. The solid was then dried and purified by a column chromatography (SiO_2, EtOAc:hexane:*i*-PrOH/90:30:3) to afford 1,3,2',6',2''',6'''-hexa-*N*-(*tert*-butoxycarbonyl)-NEO (7.41 g, 61%) as a white solid. A portion of this purified compound (4.86 g, 4.0 mmol) was dissolved in dry pyridine (40 mL) and 2,4,6-triisopropylbenzenesulfonyl chloride (TPSCl) (9.69 g, 32.0 mmol) was added. The reaction mixture was stirred at room temperature for 41 h prior to being neutralized with saturated $NaHCO_3$. The turbid liquid was extracted with EtOAc and the organic

layer was washed with brine, 0.5 M aq. HCl (twice), saturated $NaHCO_3$, and H_2O. After removal of the solvent, the crude product was purified by column chromatography (SiO_2, CH_2Cl_2:MeOH:EtOAc/100:3:3) to afford 1,3,2',6',2''',6'''-hexa-*N*-(*tert*-butoxycarbonyl)-5''-*O*-(2,4,6-triisopropylbenzenesulfonyl)-NEO (3.08 g, 51%) as a white solid. A mixture of this newly purified compound (1.46 g, 0.98 mmol), NaN_3 (0.96 g, 14.7 mmol), and DMF (15 mL) was stirred for 12 h at 80 °C. The reaction mixture was then extracted with EtOAc and washed with H_2O. After removal of the volatiles, 1,3,2',6',2''',6'''-hexa-*N*-(*tert*-butoxycarbonyl)-5''-azido-NEO (1.17 g, 96%) was obtained as white solid. A mixture of AcOH (69 μL), diisopropylethylamine (DIPEA) (209 μL) and toluene (50 mL) was stirred under Ar for 30 min. 1,3,2',6',2''',6'''-hexa-*N*-(*tert*-butoxycarbonyl)-5''-azido-NEO (744 mg, 0.6 mmol), 3,5-diethynylbenzoic acid (**4**) (51 mg, 0.3 mmol), and CuI (12 mg, 0.06 mmol) were then added to the solution. The reaction mixture was stirred for 13 h at 80 °C under Ar. The solvent was removed under reduced pressure. The residual solid was washed with Et_2O and recrystallized with CH_2Cl_2:Et_2O to give compound **5** (685 mg, 86%) as an off-white solid (Fig. 1), which was characterized after the removal of the Boc protecting group (compound **6**) (Fig. S1).

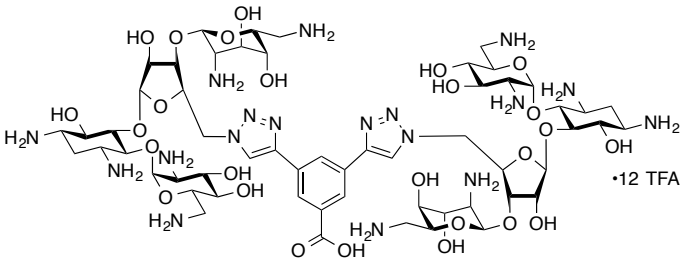

Preparation of compound 6 (DPA939) by Boc deprotection. Boc-protected NEO dimer **5** (37.1 mg, 0.014 mmol) was dissolved in a solution of TFA:H_2O/9:1 (0.7 mL). The reaction mixture was stirred at room temperature for 2 h. The solution was then poured into ice-cooled Et_2O (10 mL). The resulting precipitate was washed with Et_2O (twice) to afford the desired compound **6** (36.3 mg, 92%) as a white solid (Fig. S1A): ^{1}H NMR (500 MHz, D_2O, Figs. S2-3) δ 8.46 (s, 2H), 8.38 (s, 1H), 8.29 (d, J = 1.2 Hz, 2H), 5.92 (d, J = 3.8 Hz, 2H), 5.33 (d, J = 3.1 Hz, 2H), 5.22 (s, 2H), 4.86 (d, J = 2.8 Hz, 1H), 4.83 (d, J = 2.1 Hz, 1H), 4.74 (d, J = 6.2 Hz, 2H), 4.58-4.52 (m, 2H), 4.45 (t, J = 5.1 Hz, 2H), 4.21 (t, J = 4.9 Hz, 2H), 4.11 (t, J = 2.7 Hz, 2H), 4.00 (t, J = 9.5 Hz, 2H), 3.96 (t, J = 4.0 Hz, 2H), 3.91 (t, J = 9.5 Hz, 2H), 3.86-3.78 (m, 4H), 3.72 (s, 2H), 3.56 (t, J = 9.7 Hz, 2H), 3.51 (s, 2H), 3.47-3.39 (m, 4H), 3.37-3.19 (m, 10H), 3.18-3.08 (m, 2H), 2.43-2.30 (m, 2H), 1.78 (q, J = 12.6 Hz, 2H); ^{13}C NMR (125 MHz, D_2O, Fig. S4) δ 170.10, 163.29, 163.01, 162.72, 162.44, 146.72, 132.83, 130.98, 127.15, 126.99, 123.72, 119.95, 117.62, 115.30, 112.98, 110.33, 95.71, 94.84, 85.15, 79.79, 77.07, 75.12, 73.17, 72.42, 70.63, 70.35, 69.99, 68.08, 67.65, 67.48, 53.40, 52.21, 50.96, 49.73, 48.61, 40.56, 40.22, 27.98; MS (MALDI-TOF, Fig. S5) *m/z* calcd. for $C_{57}H_{96}N_{18}O_{26}$: 1448.67 $[M]^+$, found 1449.04.

General procedure for the synthesis of L-arginine NEO dimer conjugates 7-15 (Fig. S1B).
Step 1: Swelling of the resin (two times): Add 1.0 mL of DMF and rink amide MBHA resin (**16**) (100-200 mesh, loading 0.59 mmol/g) (13.6 mg, 0.008 mmol) to a 3 mL polypropylene cartridge with one polyethylene frit, stir for 1 min, and drain the solvent.

Step 2: Deprotection of the resin (two times): Add 0.4 mL of 25% (*v/v*) piperidine in NMP, stir for 1-2 min, and drain the solvent.

Step 3: Washing of the deprotected resin (four times): Add 0.4 mL of NMP to the resin, stirred for 5 s, and drain the solvent. This step generates resin **17**.

Step 4: Coupling reaction (one time):
Coupling of Fmoc-Arg(Pbf)-OH (Step 4a): In a vial, mix 60 μL (3 eq.) of a 0.4 M Fmoc-Arg(Pbf)-OH stock solution in NMP with the same volume (60 μL) of a 0.4 M HCTU stock solution (3 eq.). Add 8.4 μL (6 eq.) of DIPEA and thoroughly mix the resulting solution for 30 s. Add the resulting activated amino acid solution to the Fmoc-deprotected peptide resin **17** and stir at rt for 10 min. This step generates resin **18**. The Fmoc protecting group of **18** is then removed by following *Steps 2-3* to generate resin **19**. *Note*: This procedure is also used for the subsequent amino acid coupling reaction (*Step 4b*) where *Steps 1-4b* (excluding *Step 4a*) are repeated to generate resin **21**.

*Coupling of compound **5** (Step 4c) either to resin **19** to generate resin **20** or to resin **21** to generate resin **22***: In a vial, mix 60 μL (1.5 eq.) of a 0.2 M stock solution of **5** with 30 μL of a 0.4 M HCTU stock solution (1.5 eq). Add 4.2 μL (3 eq.) of DIPEA and thoroughly mix the resulting solution for 30 s. Add the resulting activated carboxylic acid solution to the Fmoc-deprotected peptide resin (**19** or **21**), stir for 20 h. This step generates either resin **20** or **22**.

After complete assembly and prior to cleavage of the product from the resin (*Step 5* below), perform a final wash of the resin with CH_2Cl_2 four times and then air-dry the resin for over 1 h.

Step 5: Cleavage of the product from the resin: Add 0.4 mL of cleavage solution (TFA:phenol:H_2O:TIPS/88:5:5:2) to the resin and stir gently for 2 h at rt. After filtration, wash the resin with 0.4 mL of TFA:H_2O/9:1. Add dropwise the filtrate to ice-cooled Et_2O (10 mL) to precipitate the desired product. Wash the solid with Et_2O (twice).

Step 6: Final purification: To a mixture of the desired product obtained in *Step 5*, add Boc_2O (33 mg, 0.15 mmol), Na_2CO_3 (16 mg, 0.15 mmol), MeOH (0.3 mL), and H_2O (0.3 mL), and stir for 4 h at rt. After adding additional H_2O (10 mL) and centrifuging, wash the precipitate with H_2O (2x 1 mL), then with Et_2O (4x 1 mL). After air drying the washed solid, dissolve it in TFA:H_2O/9:1 (0.4 mL) and stir at rt for 2 h. Add Et_2O (10 mL) to the above solution to re-precipitate the final product and wash it with Et_2O (2x 1 mL).

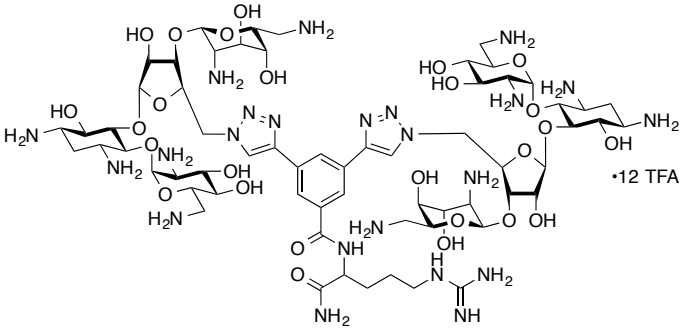

*Characterization of L-arginine NEO dimer conjugates **7-15***:
Dimer 7 (DPA930). Yield: 9.3 mg, 25%; ^{1}H NMR (300 MHz, D_2O, Fig. S6) δ 8.53 (s, 2H), 8.40 (s, 1H), 8.14 (s, 2H), 5.97 (s, 2H), 5.36 (s, 2H), 5.25 (s, 2H), 4.90-4.76 (m, 4H), 4.59-4.52 (m, 4H), 4.48-4.42 (m, 1H), 4.24 (s, 2H), 4.17-4.05 (m, 6H), 3.98-3.79 (m, 6H), 3.74 (s, 2H), 3.63 (t, *J* = 9.5 Hz, 2H), 3.53 (s, 2H), 3.50-3.38 (m, 4H), 3.37-3.24 (m, 10H), 3.17-3.06 (m,

4H), 2.47-2.28 (m, 2H), 1.93-1.76 (m, 4H), 1.72-1.58 (m, 2H); MS (MALDI-TOF, Fig. S7) *m/z* calcd. for $C_{63}H_{109}N_{23}O_{26}$: 1603.79 $[M]^+$, found 1604.07.

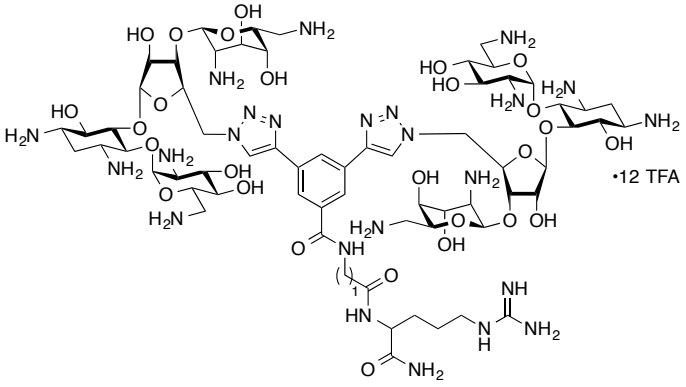

Dimer 8 (DPA931). Yield: 4.8 mg, 19%; ^{1}H NMR (500 MHz, D_2O, Fig. S8) δ 8.46 (s, 2H), 8.37 (s, 1H), 8.11 (s, 2H), 5.94 (s, 2H), 5.34 (s, 2H), 5.22 (s, 2H), 4.86-4.78 (m, 4H), 4.57-4.53 (m, 2H), 4.50 (t, *J* = 6.0 Hz, 2H), 4.22-4.20 (m, 3H), 4.15-4.08 (m, 6H), 3.97 (t, *J* = 9.0 Hz, 2H), 3.89 (t, *J* = 9.5 Hz 2H), 3.83 (t, *J* = 8.9 Hz, 4H), 3.73 (s, 2H), 3.58 (t, *J* = 9.8 Hz, 2H), 3.51 (s, 2H), 3.43-3.37 (m, 4H), 3.34-3.22 (m, 10H), 3.16-3.07 (m, 4H), 2.41-2.32 (m, 2H), 1.82-1.68 (m, 4H), 1.64-1.54 (m, 2H); MS (MALDI-TOF, Fig. S9) *m/z* calcd. for $C_{65}H_{112}N_{24}O_{27}$: 1660.81 $[M]^+$, found 1660.86.

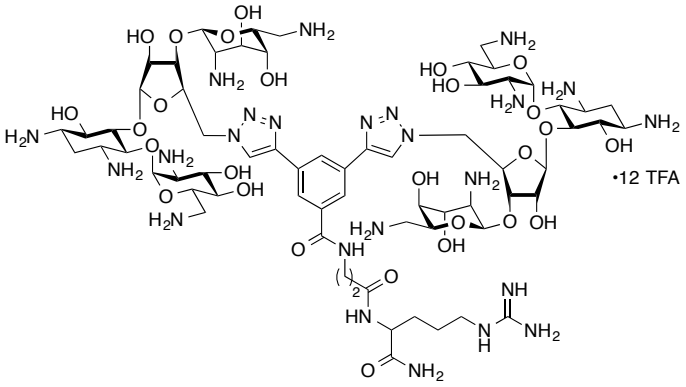

Dimer 9 (DPA932). Yield: 4.9 mg, 19%; ^{1}H NMR (500 MHz, D_2O, Fig. S10) δ 8.46 (s, 2H), 8.33 (s, 1H), 8.05 (s, 2H), 5.97 (s, 2H), 5.35 (s, 2H), 5.23 (s, 2H), 4.86-4.78 (m, 4H), 4.54 (s, 2H), 4.50 (t, *J* = 5.0 Hz, 2H), 4.22 (t, *J* = 5.0 Hz, 2H), 4.16-4.12 (m, 3H), 4.08 (s, 2H), 4.00 (t, *J* = 9.6 Hz, 2H), 3.90 (t, *J* = 9.5 Hz, 2H), 3.84 (t, *J* = 8.4 Hz, 4H), 3.73 (s, 2H), 3.63-3.57 (m, 4H), 3.51 (s, 2H), 3.47-3.41 (m, 4H), 3.35-3.24 (m, 10H), 3.17-3.11 (m, 2H), 3.00 (t, *J* = 7.2 Hz, 2H), 2.63-2.56 (m, 2H), 2.40-2.34 (m, 2H), 1.81-1.70 (m, 3H), 1.65-1.58 (m, 1H), 1.53-1.43 (m, 2H); MS (MALDI-TOF, Fig. S11) *m/z* calcd. for $C_{66}H_{114}N_{24}O_{27}$: 1674.83 $[M]^+$, found 1674.85.

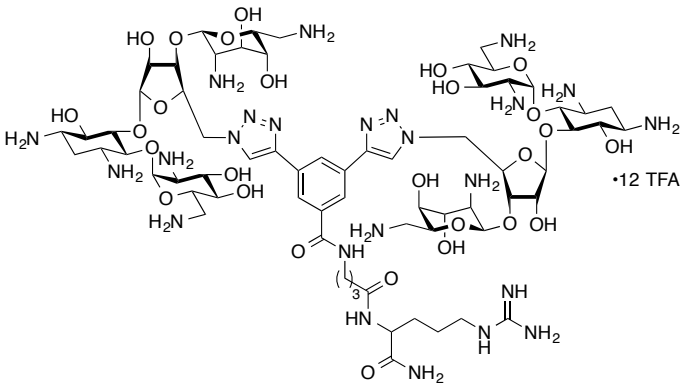

Dimer 10 (DPA933). Yield: 5.6 mg, 22%; ^{1}H NMR (500 MHz, D_2O, Fig. S12) δ 8.45 (s, 2H), 8.34 (s, 1H), 8.04 (s, 2H), 5.94 (d, *J* = 3.7 Hz, 2H), 5.34 (s, 2H), 5.22 (s, 2H), 4.85-4.78 (m, 4H), 4.55-4.52 (m, 2H), 4.50 (t, *J* = 5.0 Hz, 2H), 4.21 (t, *J* = 5.0 Hz, 2H), 4.14-4.07 (m, 5H), 3.95 (t, *J* = 9.0 Hz, 2H), 3.90 (t, *J* = 10.2 Hz, 2H), 3.86-3.80 (m, 4H), 3.72 (s, 2H), 3.57 (t, *J* = 9.5 Hz, 2H), 3.51 (s, 2H), 3.44-3.40 (m, 2H), 3.39-3.28 (m, 12H), 3.27-3.22 (m, 2H), 3.15-3.08 (m, 2H), 3.05 (t, *J* = 6.9 Hz, 2H), 2.40-2.28 (m, 4H), 1.88-1.81 (m, 2H), 1.77-1.69 (m, 2H), 1.68-1.42 (m, 4H); MS (MALDI-TOF, Fig. S13) *m/z* calcd. for $C_{67}H_{116}N_{24}O_{27}$: 1688.84 $[M]^+$, found 1688.71.

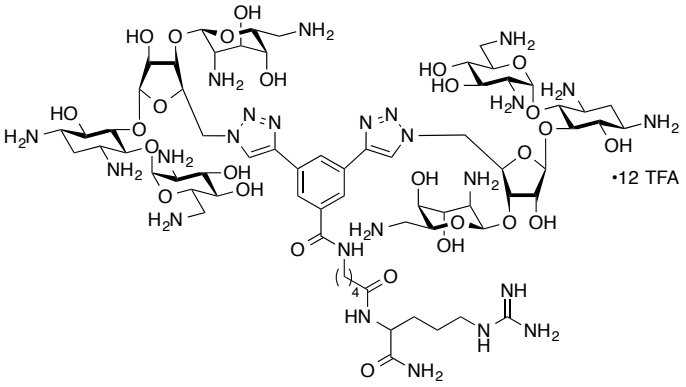

Dimer 11 (DPA934). Yield: 5.2 mg, 20%; ^{1}H NMR (500 MHz, D_2O, Fig. S14) δ 8.45 (s, 2H), 8.33 (s, 1H), 8.04 (s, 2H), 5.95 (d, *J* = 2.7 Hz, 2H), 5.34 (s, 2H), 5.23 (s, 2H), 4.86-4.74 (m, 4H), 4.57-4.52 (m, 2H), 4.49 (t, *J* = 5.0 Hz, 2H), 4.22 (t, *J* = 4.6 Hz, 2H), 4.14-4.11 (m, 3H), 4.08 (s, 2H), 3.99 (t, *J* = 9.6 Hz, 2H), 3.91 (t, *J* = 9.7 Hz, 2H), 3.84 (t, *J* = 8.2 Hz, 4H), 3.73 (s, 2H), 3.58 (t, *J* = 9.7 Hz, 2H), 3.51 (s, 2H), 3.45-3.38 (m, 4H), 3.36-3.24 (m, 12H), 3.15-3.10 (m, 2H), 3.08 (t, *J* = 6.9 Hz, 2H), 2.40-2.33 (m, 2H), 2.27 (t, *J* = 6.8 Hz, 2H), 1.79-1.67 (m, 3H), 1.65-1.52 (m, 7H); MS (MALDI-TOF, Fig. S15) *m/z* calcd. for $C_{68}H_{118}N_{24}O_{27}$: 1702.86 $[M]^+$, found 1702.85.

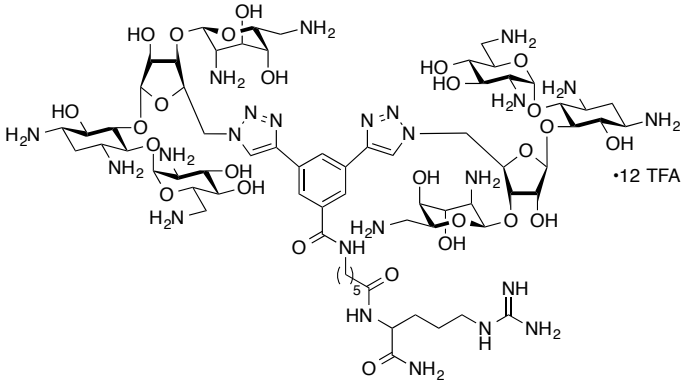

Dimer 12 (DPA935). Yield: 5.1 mg, 20%; ^{1}H NMR (500 MHz, D_2O, Fig. S16) δ 8.45 (s, 2H), 8.32 (s, 1H), 8.03 (s, 2H), 5.96 (d, *J* = 2.6 Hz, 2H), 5.34 (s, 2H), 5.23 (s, 2H), 4.85-4.78 (m, 4H), 4.54 (s, 2H), 4.49 (t, *J* = 5.0 Hz, 2H), 4.22 (t, *J* = 4.9 Hz, 2H), 4.14-4.08 (m, 3H), 4.06 (s, 2H), 4.00 (t, *J* = 9.4 Hz, 2H), 3.91 (t, *J* = 9.9 Hz, 2H), 3.84 (t, *J* = 8.3 Hz, 4H), 3.73 (s, 2H), 3.58 (t, *J* = 9.6 Hz, 2H), 3.51 (s, 2H), 3.48-3.40 (m, 4H), 3.36-3.22 (m, 12H), 3.17-3.10 (m, 2H), 3.04 (t, *J* = 6.5 Hz, 2H), 2.43-2.33 (m, 2H), 2.22 (t, *J* = 7.1 Hz, 2H), 1.83-1.73 (m, 2H), 1.73-1.65 (m, 1H), 1.62-1.45 (m, 7H), 1.34-1.25 (m, 2H); MS (MALDI-TOF, Fig. S17) *m/z* calcd. for $C_{69}H_{120}N_{24}O_{27}$: 1716.88 $[M]^+$, found 1716.88.

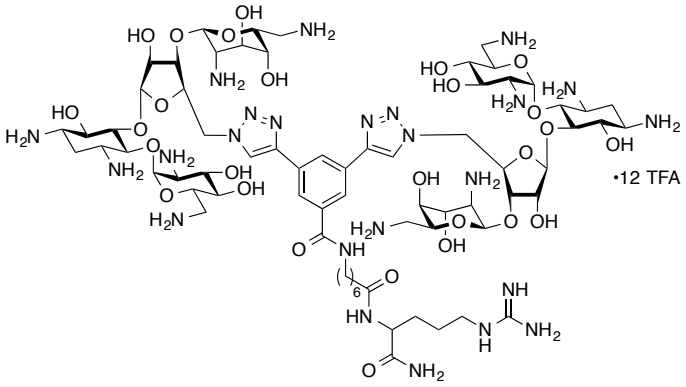

Dimer 13 (DPA936). Yield: 5.5 mg, 21%; ^{1}H NMR (500 MHz, D_2O, Fig. S18) δ 8.45 (s, 2H), 8.32 (s, 1H), 8.04 (s, 2H), 5.96 (d, *J* = 3.4 Hz, 2H), 5.34 (s, 2H), 5.23 (s, 2H), 4.85-4.78 (m, 4H), 4.55 (s, 2H), 4.49 (t, *J* = 5.0 Hz, 2H), 4.22 (t, *J* = 4.0 Hz, 2H), 4.15-4.10 (m, 3H), 4.07 (t, *J* = 5.0 Hz, 2H), 4.00 (t, *J* = 9.5 Hz, 2H), 3.91 (t, *J* = 9.5 Hz, 2H), 3.84 (t, *J* = 8.8 Hz, 4H), 3.73 (s, 2H), 3.58 (t, *J* = 9.7 Hz, 2H), 3.51 (s, 2H), 3.47-3.40 (m, 4H), 3.38-3.24 (m, 12H), 3.16-3.10 (m, 2H), 3.08 (t, *J* = 6.4 Hz, 2H), 2.47-2.27 (m, 2H), 2.20 (t, *J* = 7.5 Hz, 2H), 1.82-1.67 (m, 3H), 1.63-1.46 (m, 7H), 1.34-1.22 (m, 4H); MS (MALDI-TOF, Fig. S19) *m/z* calcd. for $C_{70}H_{122}N_{24}O_{27}$: 1730.89 $[M]^+$, found 1730.79.

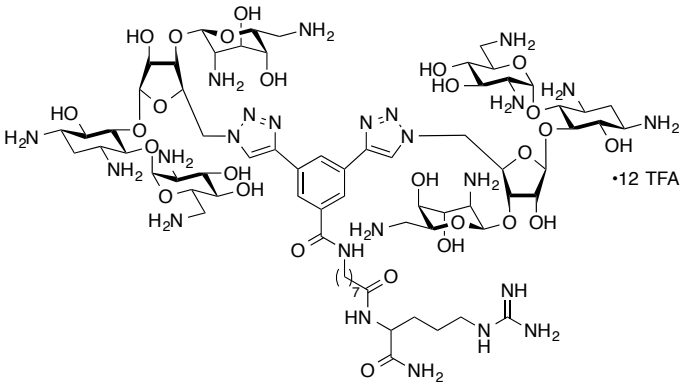

Dimer 14 (DPA937). Yield: 5.3 mg, 21%; ^{1}H NMR (500 MHz, D_2O, Fig. S20) δ 8.45 (s, 2H), 8.32 (s, 1H), 8.03 (s, 2H), 5.95 (d, *J* = 2.8 Hz, 2H), 5.34 (s, 2H), 5.22 (s, 2H), 4.85-4.78 (m, 4H), 4.56-4.51 (m, 2H), 4.49 (t, *J* = 5.0 Hz, 2H), 4.22 (t, *J* = 5.0 Hz, 2H), 4.14-4.10 (m, 3H), 4.07 (s, 2H), 3.99 (t, *J* = 9.6 Hz, 2H), 3.90 (t, *J* = 9.7 Hz, 2H), 3.83 (t, *J* = 8.6 Hz, 4H), 3.73 (s, 2H), 3.58 (t, *J* = 9.6 Hz, 2H), 3.51 (s, 2H), 3.47-3.39 (m, 4H), 3.35-3.22 (m, 12H), 3.16-3.10 (m, 2H), 3.07 (t, *J* = 6.4 Hz, 2H), 2.43-2.30 (m, 2H), 2.18 (t, *J* = 7.2 Hz, 2H), 1.83-1.66 (m, 3H), 1.62-1.45 (m, 7H), 1.30-1.17 (m, 6H); MS (MALDI-TOF, Fig. S21) *m/z* calcd. for $C_{71}H_{124}N_{24}O_{27}$: 1744.91 $[M]^+$, found 1744.94.

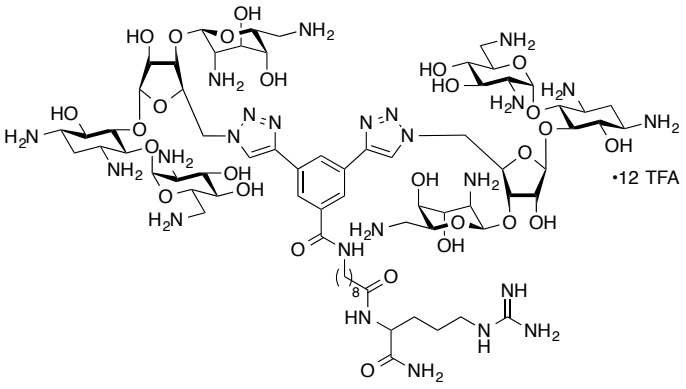

Dimer 15 (DPA938). Yield: 6.7 mg, 26%; ^{1}H NMR (500 MHz, D_2O, Fig. S22) δ 8.45 (s, 2H), 8.32 (s, 1H), 8.04 (s, 2H), 5.95 (d, *J* = 3.6 Hz, 2H), 5.34 (d, *J* = 2.9 Hz, 2H), 5.22 (s, 2H), 4.82-4.78 (m, 4H), 4.54 (s, 2H), 4.49 (t, *J* = 5.0 Hz, 2H), 4.21 (t, *J* = 5.0 Hz, 2H), 4.14-4.09 (m, 3H), 4.06 (t, *J* = 4.0 Hz, 2H), 3.99 (t, *J* = 9.5 Hz, 2H), 3.91 (t, *J* = 9.5 Hz, 2H), 3.83 (t, *J* = 8.3 Hz, 4H), 3.72 (s, 2H), 3.58 (t, *J* = 9.7 Hz, 2H), 3.51 (s, 2H), 3.47-3.39 (m, 4H), 3.36-3.21 (m, 12H), 3.16-3.10 (m, 2H), 3.07 (t, *J* = 6.7 Hz, 2H), 2.42-2.31 (m, 2H), 2.14 (t, *J* = 7.0 Hz, 2H), 1.81-1.65 (m, 3H), 1.59-1.40 (m, 7H), 1.26-1.10 (m, 14H); MS (MALDI-TOF, Fig. S23) *m/z* calcd. for $C_{75}H_{132}N_{24}O_{27}$: 1800.97 $[M]^+$, found 1800.73.

Biochemical and biological studies:

***E. coli* and human ribosomal RNA A-site binding.**

Determination of dissociation constant between F-NEO and A-sites. Titrations of F-NEO with A-site models were used to calculate dissociation constants (K_d). The observed emission, *I*, is the combination emission intensities from bound, I_b, and free F-NEO, I_f:

$$I = I_b \times [F-NEO]_b + I_f \times [F-NEO]_f$$

Using mass balance, K_d can be calculated from equation that describes the relationship between in $[F\text{-}NEO]_b$ and added RNA, $[RNA]_{total}$:

$$[F-NEO]_b^2 - ([F-NEO]_{total} + [RNA]_{total} + K_d) + [F-NEO]_{total} \times [RNA]_{total} = 0$$

[F-NEO]$_{total}$ and *[RNA]$_{total}$* are the total concentrations of F-NEO and [RNA] in the well.

Screening of compounds 6-16. Compounds **6-15** and a control molecule **16** (DPA 928) (Fig. 1C) were initially screened using an F-NEO competitive binding assay as previously described[4] with few modifications. Each compound at 0.1 μM concentration was added to 0.1 μM F-NEO:A-site complex to a final volume of 200 μL. The displacement of F-NEO by test compounds was measured by an increase of emission relatively to F-NEO:A-site complex alone (ΔF). The percentage of displacement was calculated using equation 1 relatively to the fluorescence of 0.1 μM F-NEO ($\Delta F_{F\text{-}NEO}$):

$$\% \text{ displacement} = (\Delta F/\Delta F_{F\text{-}NEO})\times 100 \qquad \text{(equation 1)}$$

IC_{50} measurements. IC_{50} values for compounds **6-15** were determined by titrations of F-NEO-A-site complex at 0.1 μM concentrations with increasing concentrations of tested compounds ranging from 0.002 μM to 2.0 μM. All titrations were performed in a black 96-well round-bottom plate (Greiner). Emission intensity was measured using 25 reads/well with an Infinite M1000 Pro (Tecan) plate reader ($\lambda_{ex/em}$ = 485/535 nm). All experiments were performed at least in duplicates using 10 mM HEPES, 50 mM NaCl, and 0.4 mM EDTA at pH 7.0. Graphs for the determination of IC_{50} values against *E. coli* and human are presented in Figs. S24 and S25, respectively.

Determination of selectivity factors. This calculation is intended for a quick and convenient estimation of binding preferences of a compound (*cpd*) to one A-site *versus* another. We conduct an exchange reaction between A-site – F-NEO complex and a compound with binding constant $K_{E.\ coli}$ for *E. coli* A-site and K_{human} for human A-site:

$$A-site \bullet F-NEO + cpd \rightleftharpoons A-site \bullet cpd + F-NEO$$

The following relationship is true:

$$\frac{K_{\text{human}}}{K_{E.\ coli}} = \frac{K_d^{F-NEO}(\text{human})}{K_d^{F-NEO}(E.coli)} \times \frac{K_d^{cpd}(E.coli)}{K_d^{cpd}(\text{human})}$$

Where $K_d^{\text{F-NEO}}$ (*E. coli*) and $K_d^{\text{F-NEO}}$ (human) are dissociation constants between F-NEO and *E. coli* and human A-sites, respectively, and K_d^{cpd}(*E. coli*) and K_d^{cpd} (human) are dissociation constants between a compound and *E. coli* and human A-sites, respectively.
After regrouping:

$$\frac{K_d^{cpd}(\text{human})}{K_d^{cpd}(E.coli)} = 5.75\times\frac{K_{E.\ coli}}{K_{\text{human}}}$$

Measurement of $K_{E.\ coli}$ and K_{human} is not possible under our experimental conditions (for example, utilized concentrations, signal detection etc), therefore we substitute *K* with conveniently measured IC_{50}, a total concentration of compound or NEO, at which the emission intensity at half of the maximum value is observed. Higher IC_{50} value corresponds to a lower binding affinity when IC_{50} values for the same A-site are considered. After substitution of the ratio $K_{E.}$

$_{coli}/K_{human}$ by IC_{50} (human)/IC_{50} (*E. coli*), we can calculate selectivity factor representing the approximation of the binding preference of a compound to *E. coli* over human A-site:

$$Selectivity\ factor = 5.75 \times \frac{IC_{50}\ (\text{human})}{IC_{50}\ (E.coli)}$$

Determination of MIC values for compounds 6-15. *B. cereus* ATCC 11778, *S. epidermidis* ATCC 12228, *S. aureus* ATCC 25923 were purchased from ATCC (Manassas, VA, USA). Compounds **6-15** and NEO were serially diluted 2-fold to make 50 μM to 0.098 μM final concentrations. Bacterial strains were grown in LB for 24 h (250 rpm, 37 °C). Overnight bacterial culture was diluted to 1:1000, grown for 4 h, diluted again 1:1000, and added to the microplates. Plates were incubated at 37 °C for 16-20 h and inspected visually and with MTT (50 μL of 1 mg/mL).

Determination of aminoglycoside-modifying enzymes (AMEs) activity on compounds 6-15. The *N*-acetylation and *O*-phosphorylation of compounds **6-15** by AMEs was examined as previously described.[5-7] All reactions were monitored at 37 °C (AAC(6')-Ie/APH(2")-Ia only) or 25 °C on a SpectraMax M5 microplate reader and performed in triplicate. All rates were normalized to that of NEO. All acetylation reactions were monitored using Ellman's method at 412 nm (ε = 14,150 $M^{-1}cm^{-1}$) using 2 mM DTNB, 150 μM AcCoA (except for Eis where 500 μM was used), 50 mM of the appropriate buffer (except for AAC(2')-Ic where 100 mM was used), 100 μM compounds **6-15**, and 0.125 μM (AAC(2')-Ic and AAC(3)-IV) or 0.5 μM (all other AACs) enzyme. Phosphorylation using NADH (0.5 mg/mL) in re-generation of GTP was monitored at 324 nm (ε = 6,220 $M^{-1}cm^{-1}$). Reactions contained 1 μM APH(2")-Ia or APH(3')-Ia, 2 mM GTP, and 100 μM compounds **6-15**.

Docking of dimer 11 with RNA A-sites. The 3D structure of compound **11** was obtained using ChemDraw 12.0. Atomic coordinates of the receptor for the docking with the *E. coli* RNA A-site as well as the human RNA A-site have been extracted from the crystal structures from PDB ID 2A04[8] and 2FQN,[9] respectively. The structure of compound **11** and the receptors were prepared for docking using AutoDock Tools Suite version 1.3.2.[10] All structures were viewed in UCSF Chimera[11] and then brought to their energetically minimized structures by Gaussian utilizing a conjugate gradient method with a 6-31G MP2 force field. AutoDock Tools (ADT) were used to merge nonpolar hydrogen atoms of both RNAs and assign atomic charges. Nonpolar hydrogen atoms of each compound were merged and rotatable bonds were assigned. Grid maps were generated for each atom type using AUTOGRID. An active site box of 70 × 70 × 70 $Å^3$ with grid spacing of 0.375 Å was created and placed at the center of RNA structures. Docking calculations were carried out using Lamarckian genetic algorithm. A population of random individuals (population size: 150) was used with 2,500,000 energy evaluations. A maximum number of 27,000 generations with mutation rate of 0.02 were used. Fifty independent runs for each compound were performed with each RNA A-site. The resulting positions were clustered according to a root-mean-square criterion of 0.5 Å.

References:

[1] Xi, H., Davis, E., Ranjan, N., Xue, L., Hyde-Volpe, D., and Arya, D. P. (2011) Thermodynamics of nucleic acid "shape readout" by an aminosugar, *Biochemistry*, *50*, 9088-9113.

[2] Kissel, P., Breitler, S., Reinmuller, V., Lanz, P., Federer, L., Schluter, A. D., and Sakamoto, J. (2009) An easy and multigram-scale synthesis of versatile AA- and AB-type *m*-terphenylenes as building blocks for kinked polyphenylenes, *Eur. J. Org. Chem.*, 2953-2955.

[3] Smeyanov, A., and Schmidt, A. (2013) K3PO4-KOH Mixture as Efficient Reagent for the deprotection of 4-aryl-2-methyl-3-butyn-2-ols to terminal acetylenes, *Synthetic Comm.*, *43*, 2809-2816.

[4] Watkins, D., Norris, F. A., Kumar, S., and Arya, D. P. (2013) A fluorescence-based screen for ribosome binding antibiotics, *Anal. Biochem.*, *434*, 300-307.

[5] Green, K. D., Chen, W., Houghton, J. L., Fridman, M., and Garneau-Tsodikova, S. (2010) Exploring the substrate promiscuity of drug-modifying enzymes for the chemoenzymatic generation of *N*-acylated aminoglycosides, *ChemBioChem*, *11*, 119-126.

[6] Green, K. D., Chen, W., and Garneau-Tsodikova, S. (2011) Effects of altering aminoglycoside structures on bacterial resistance enzyme activities, *Antimicrob. Agents Chemother.*, *55*, 3207-3213.

[7] Chen, W., Biswas, T., Porter, V. R., Tsodikov, O. V., and Garneau-Tsodikova, S. (2011) Unusual regioversatility of acetyltransferase Eis, a cause of drug resistance in XDR-TB, *Proc. Natl. Acad. Sci., U. S. A.*, *108*, 9804-9808.

[8] Zhao, F., Zhao, Q., Blount, K. F., Han, Q., Tor, Y., and Hermann, T. (2005) Molecular recognition of RNA by neomycin and a restricted neomycin derivative, *Angew. Chem.*, *44*, 5329-5334.

[9] Kondo, J., Urzhumtsev, A., and Westhof, E. (2006) Two conformational states in the crystal structure of the *Homo sapiens* cytoplasmic ribosomal decoding A-site, *Nucl. Acids Res.*, *34*, 676-685.

[10] Sandeep, G., Nagasree, K. P., Hanisha, M., and Kumar, M. M. (2011) AUDocker LE: A GUI for virtual screening with AUTODOCK Vina, *BMC Res. Notes*, *4*, 445.

[11] Pettersen, E. F., Goddard, T. D., Huang, C. C., Couch, G. S., Greenblatt, D. M., Meng, E. C., and Ferrin, T. E. (2004) UCSF Chimera--a visualization system for exploratory research and analysis, *J. Comp. Chem.*, *25*, 1605-1612.

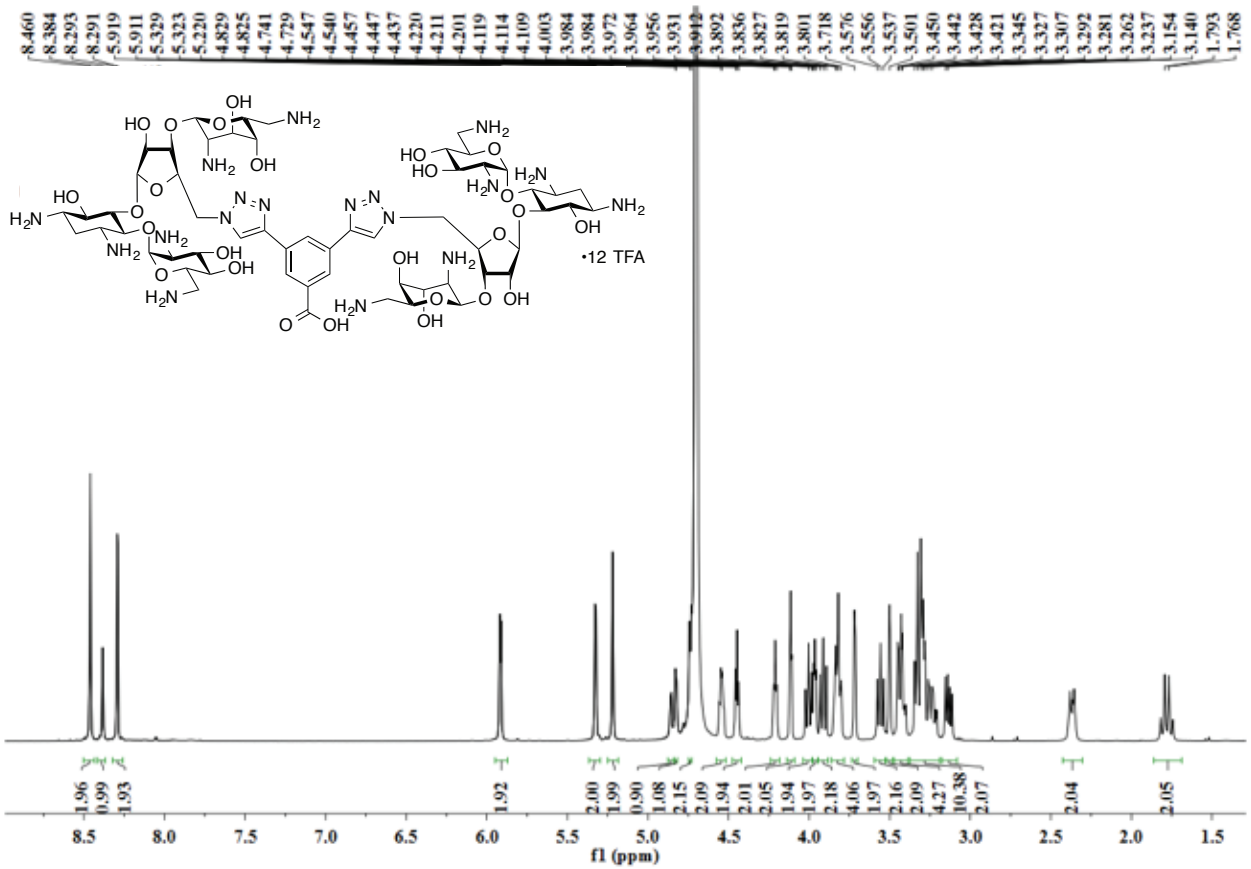

Fig. S2. ^{1}H NMR spectrum of compound **6** in D_2O.

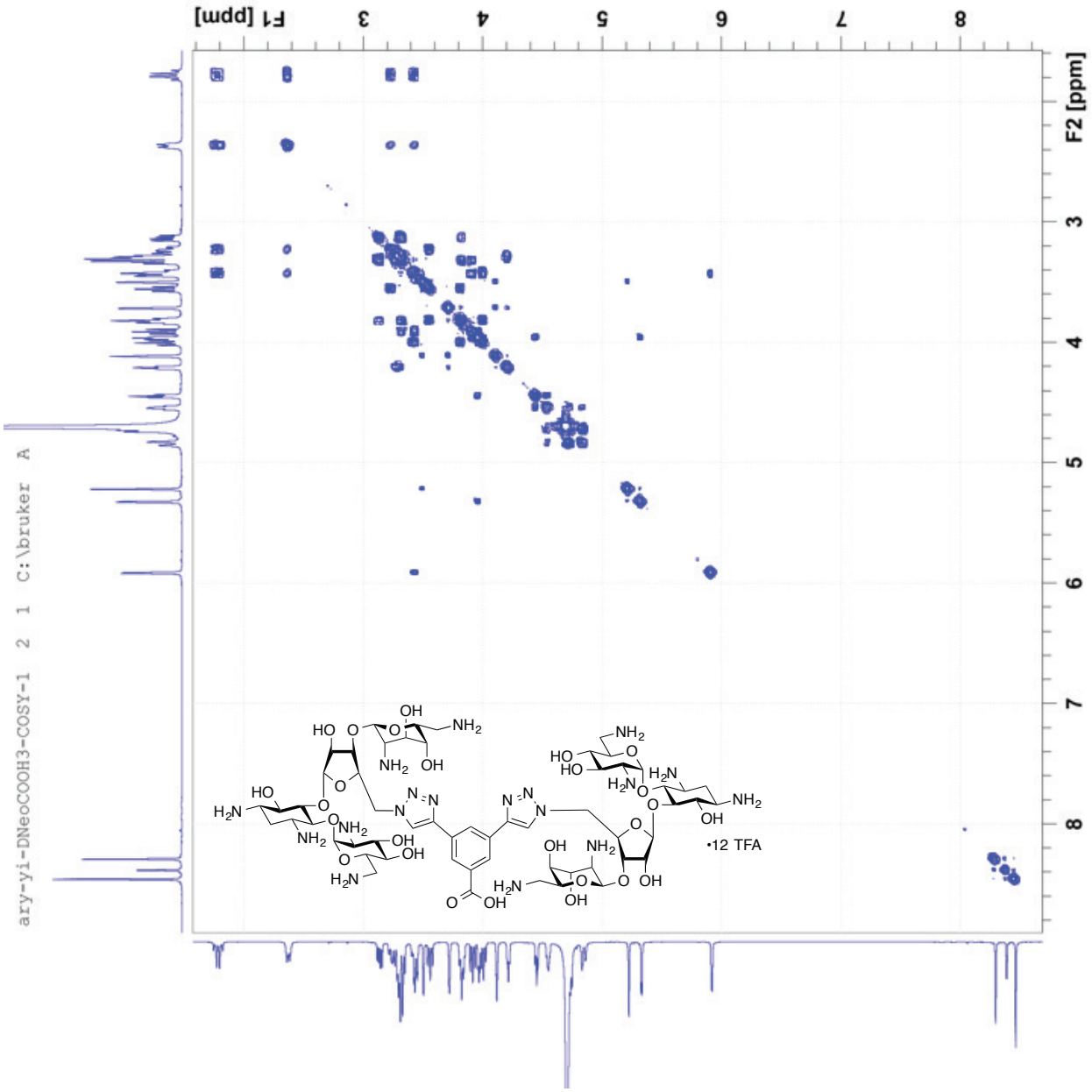

Fig. S3. COSY spectrum of compound **6** in D_2O.

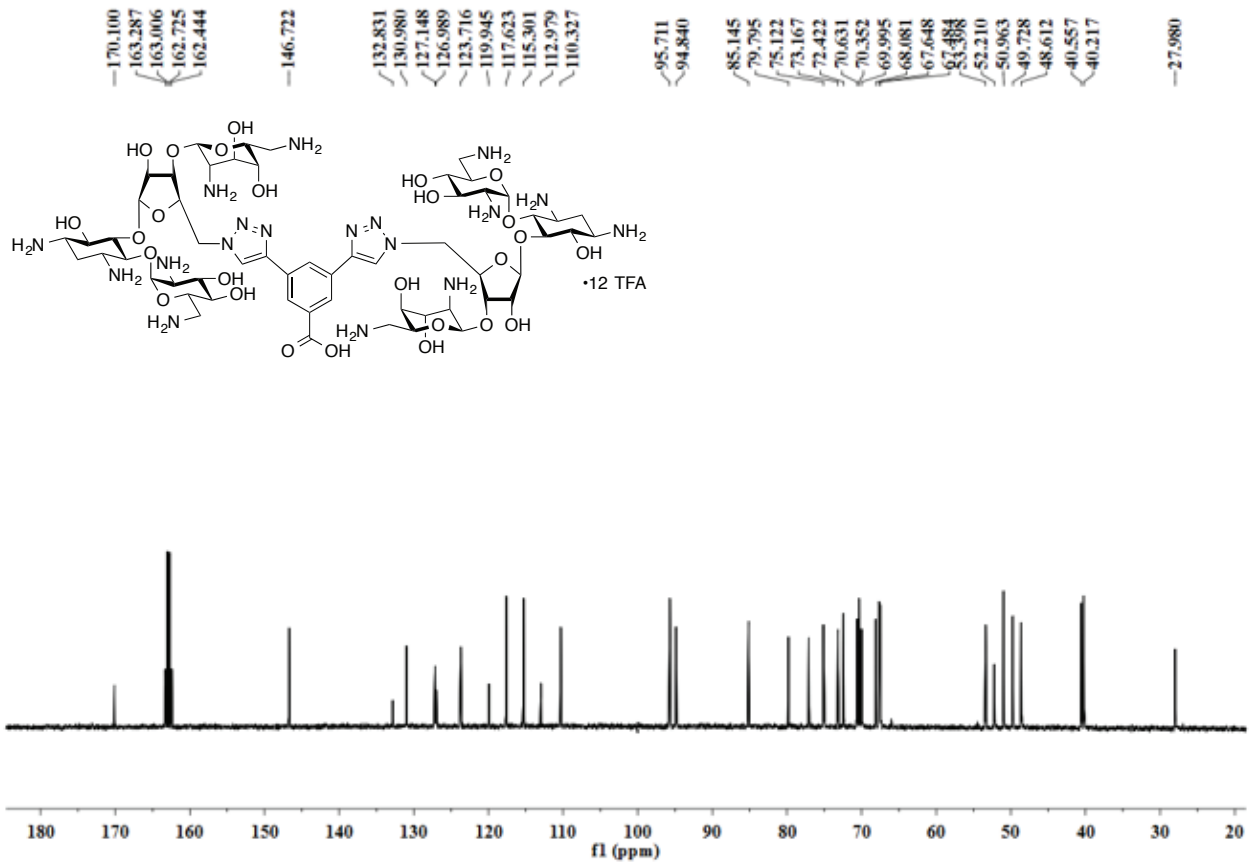

Fig. S4. ^{13}C NMR spectrum of compound **6** in D_2O.

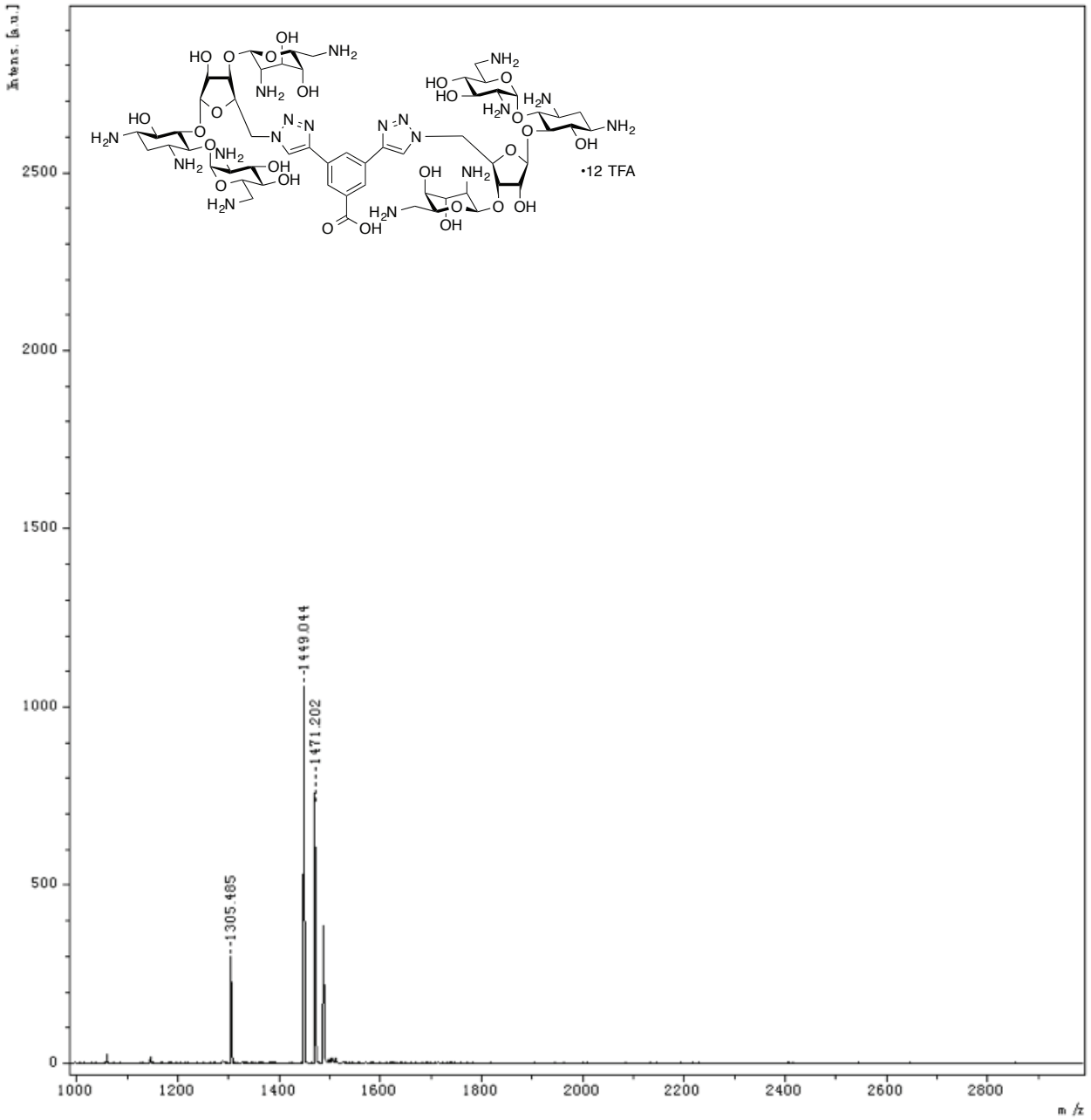

Fig. S5. MALDI-TOF MS of compound **6**.

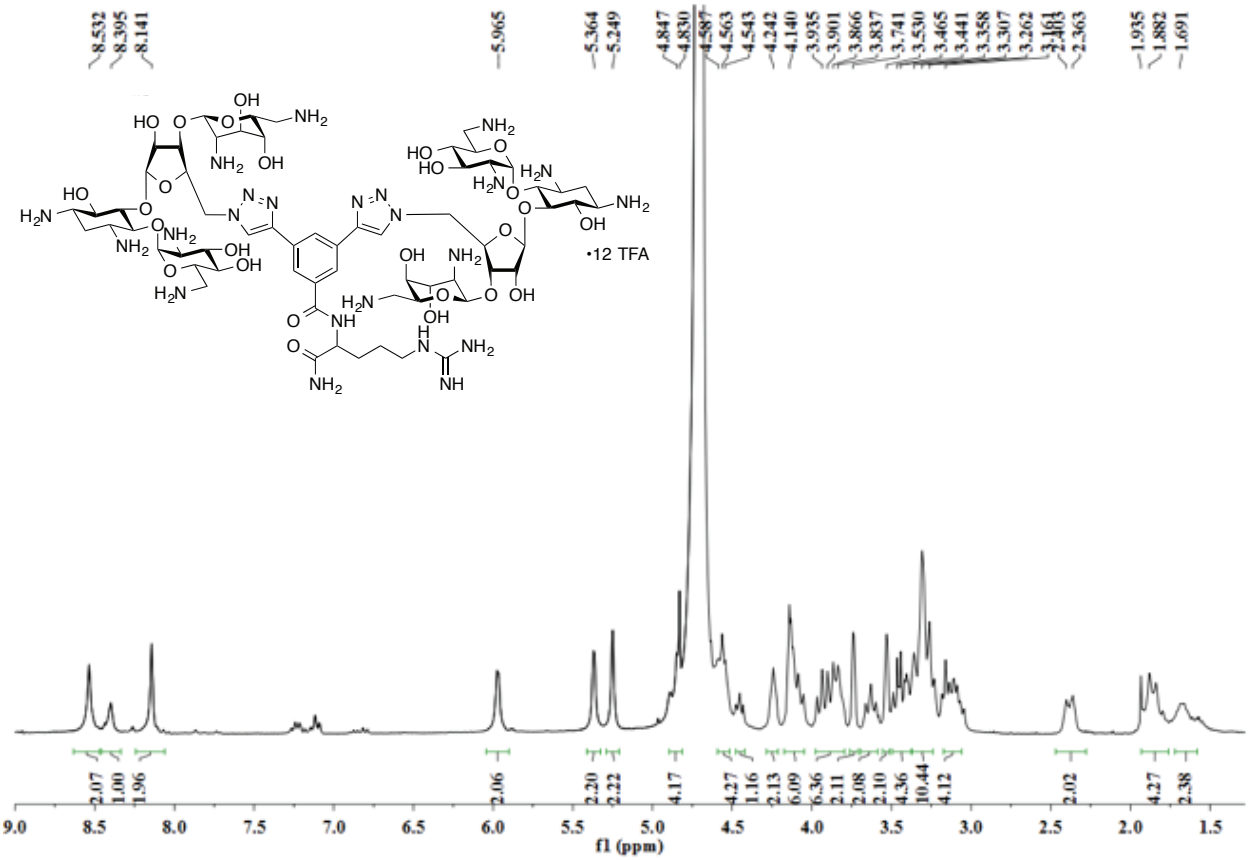

Fig. S6. ^{1}H NMR spectrum of compound **7** in D_2O.

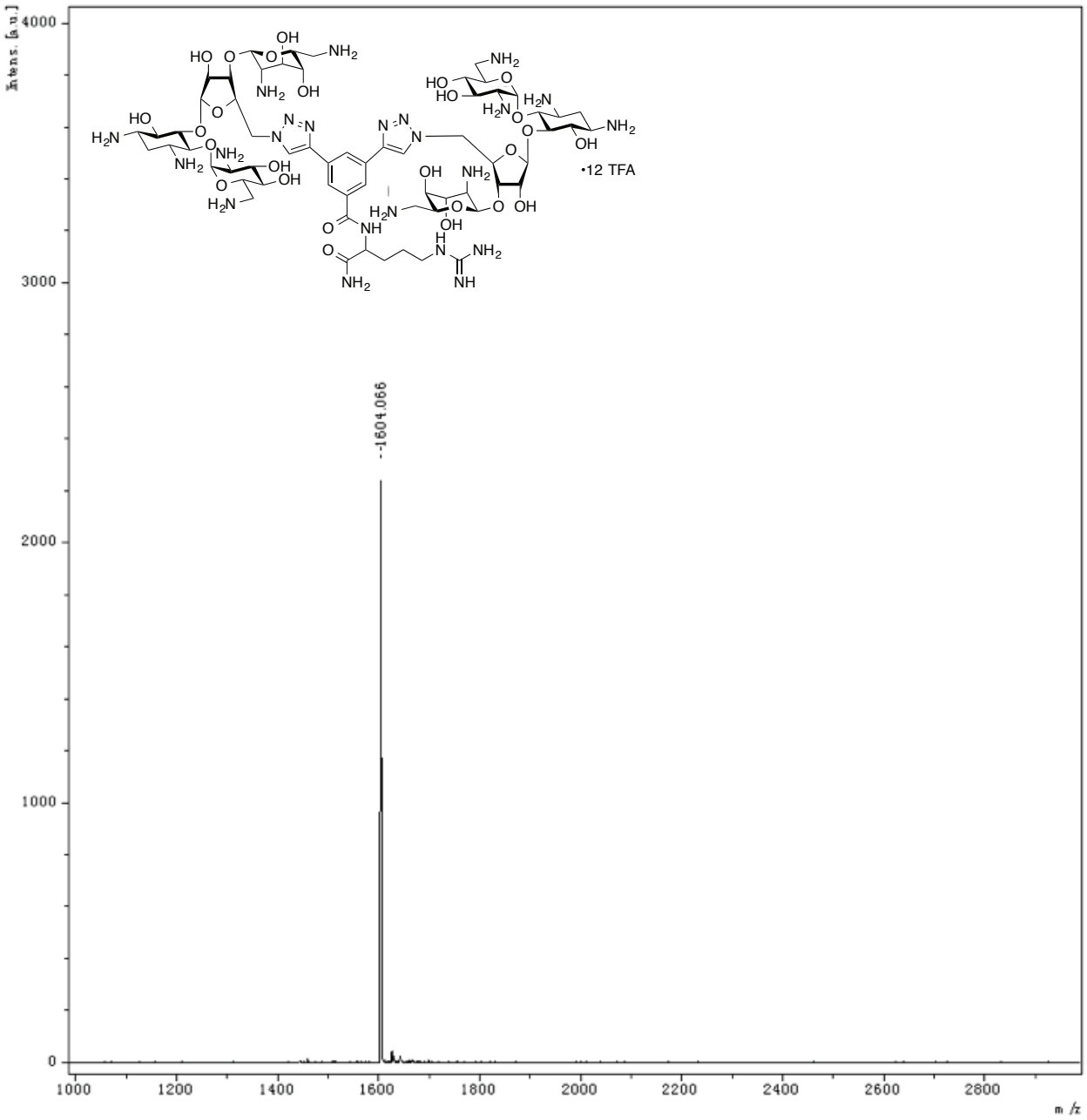

Fig. S7. MALDI-TOF MS of compound **7**.

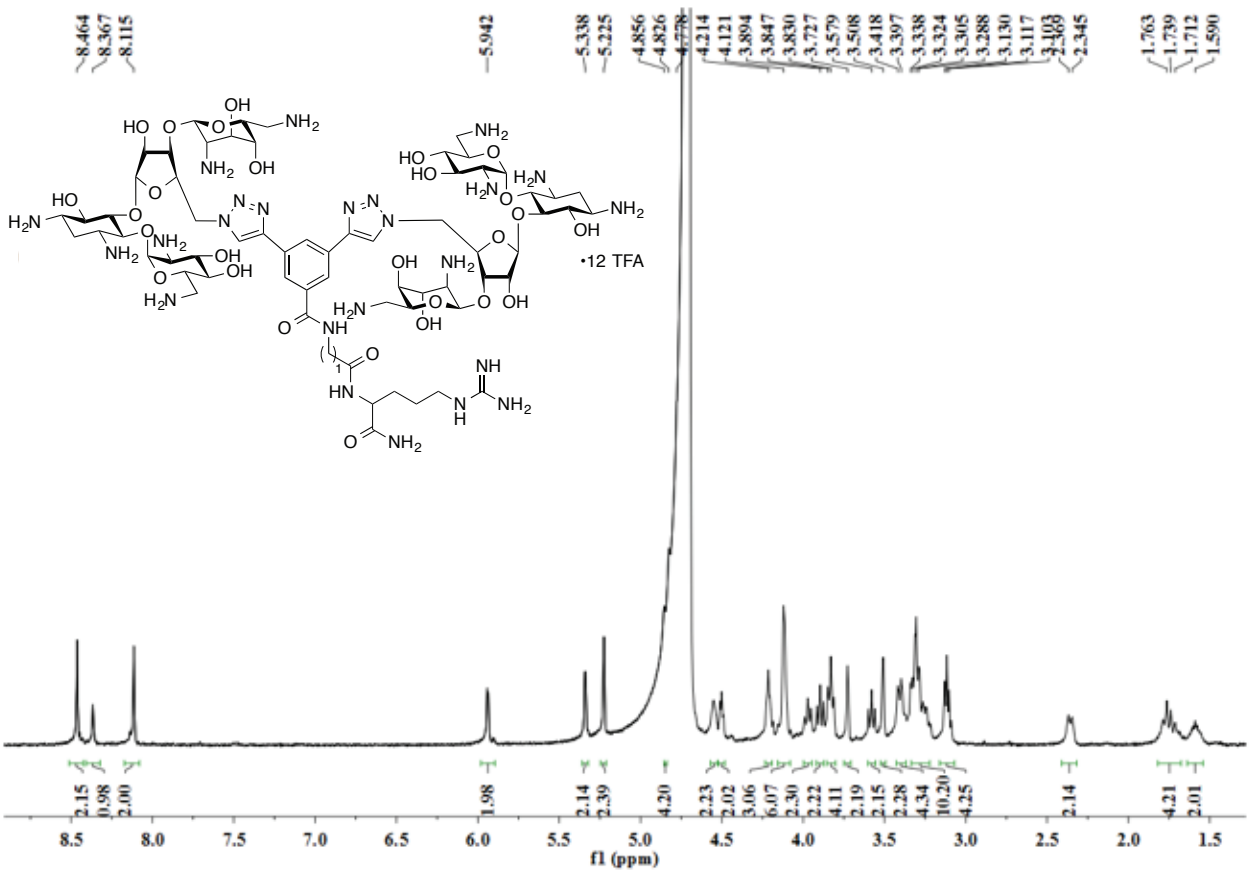

Fig. S8. ^{1}H NMR spectrum of compound **8** in D_2O.

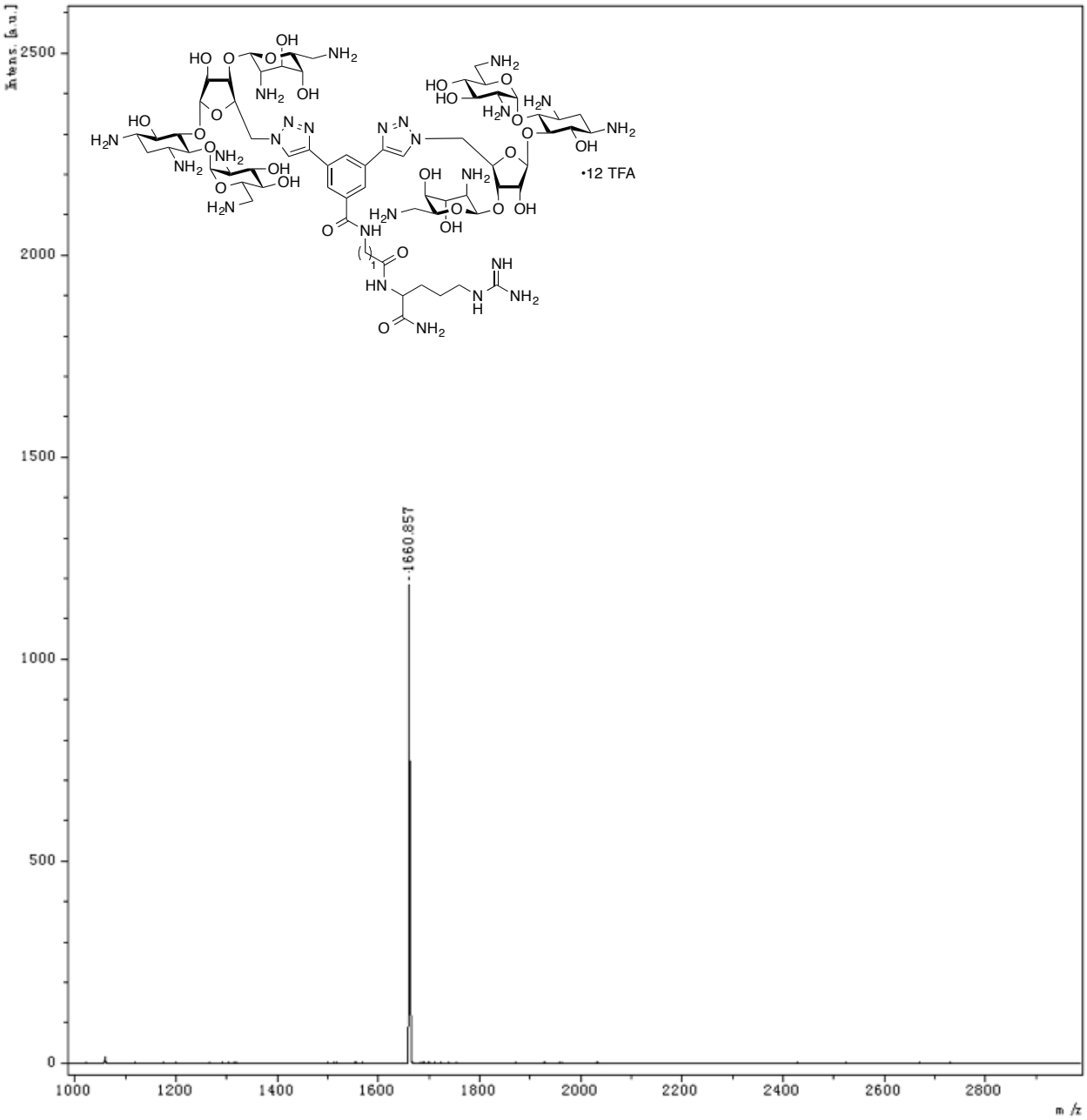

Fig. S9. MALDI-TOF MS of compound **8**.

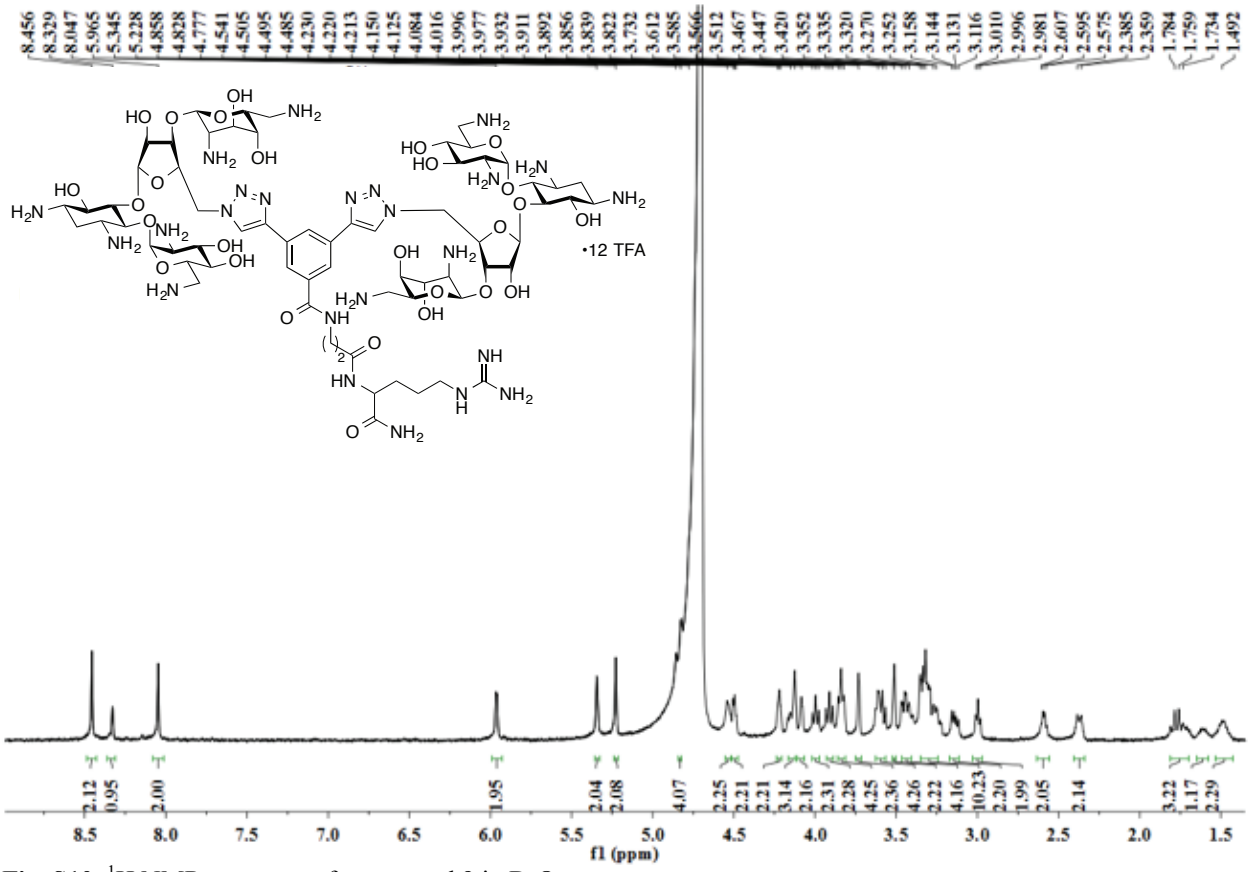

Fig. S10. ^{1}H NMR spectrum of compound **9** in D_2O.

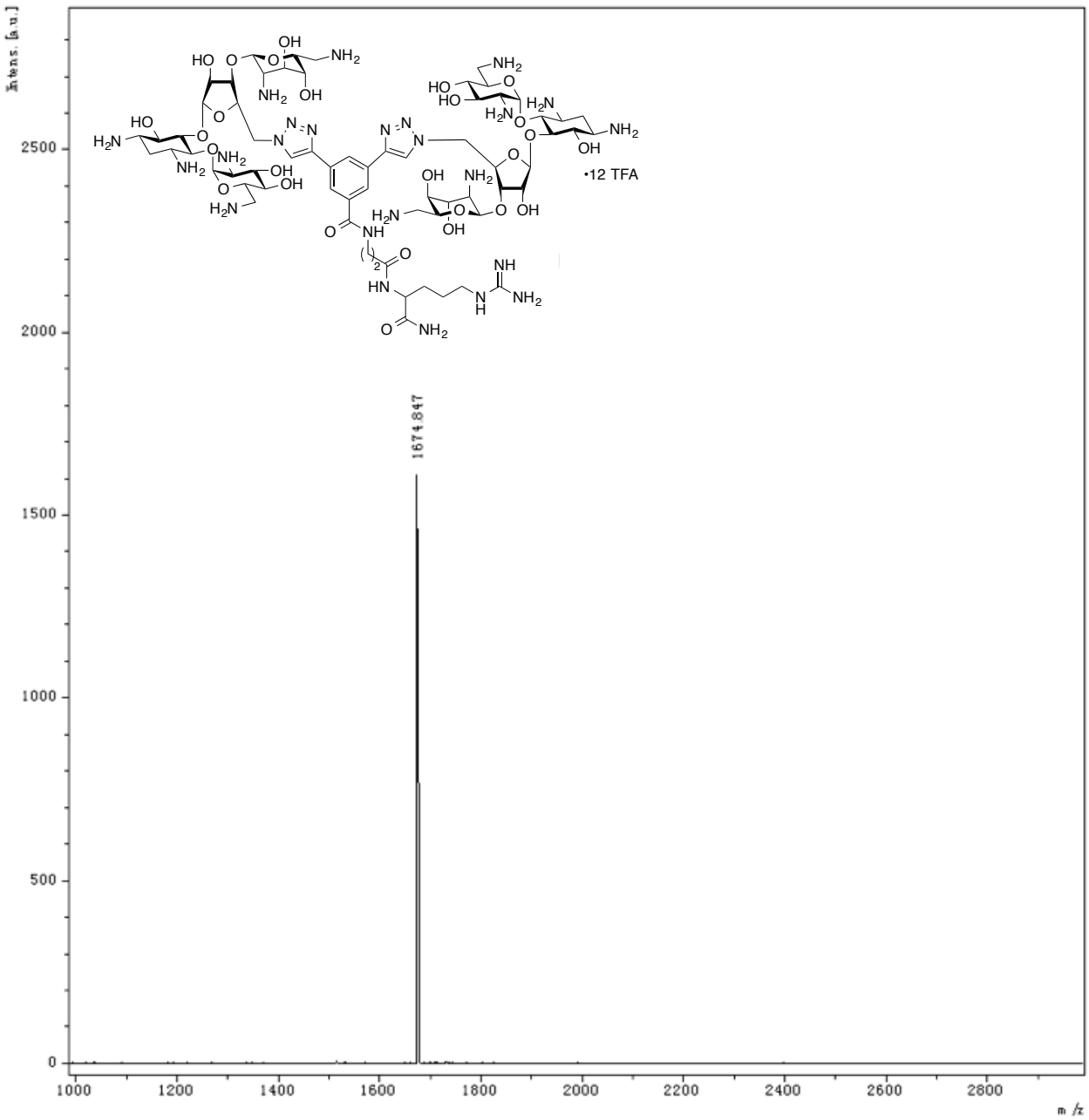

Fig. S11. MALDI-TOF MS of compound **9**.

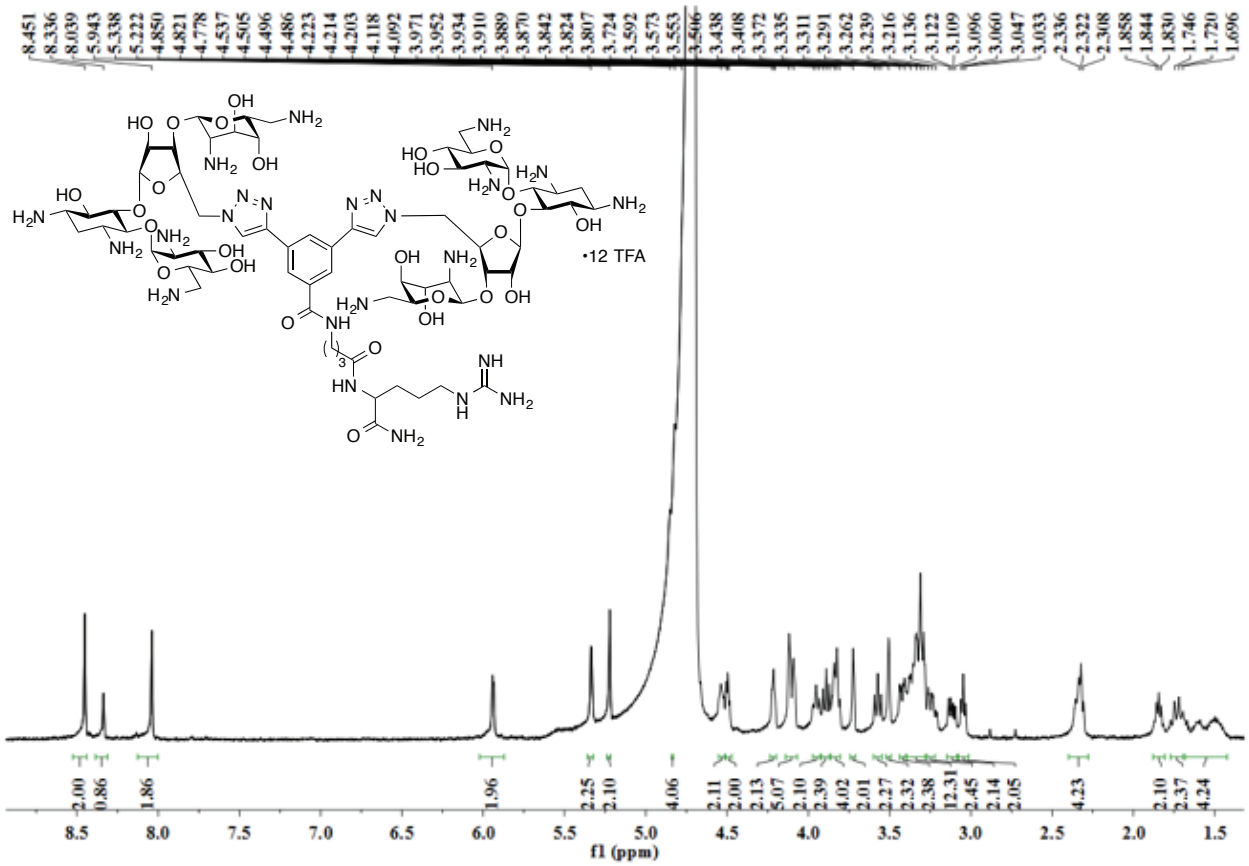

Fig. S12. ^{1}H NMR spectrum of compound **10** in D_2O.

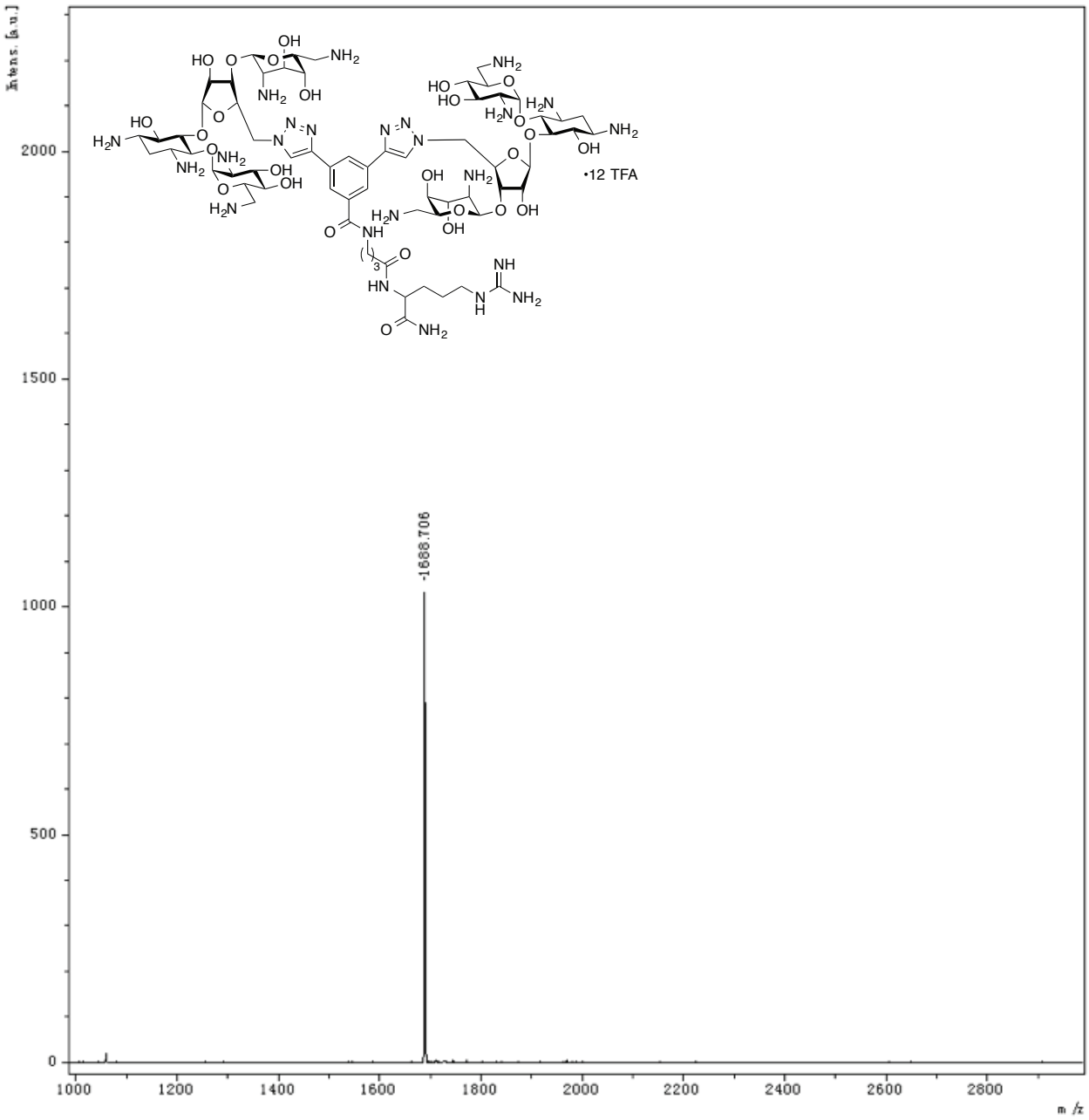

Fig. S13. MALDI-TOF MS of compound **10**.

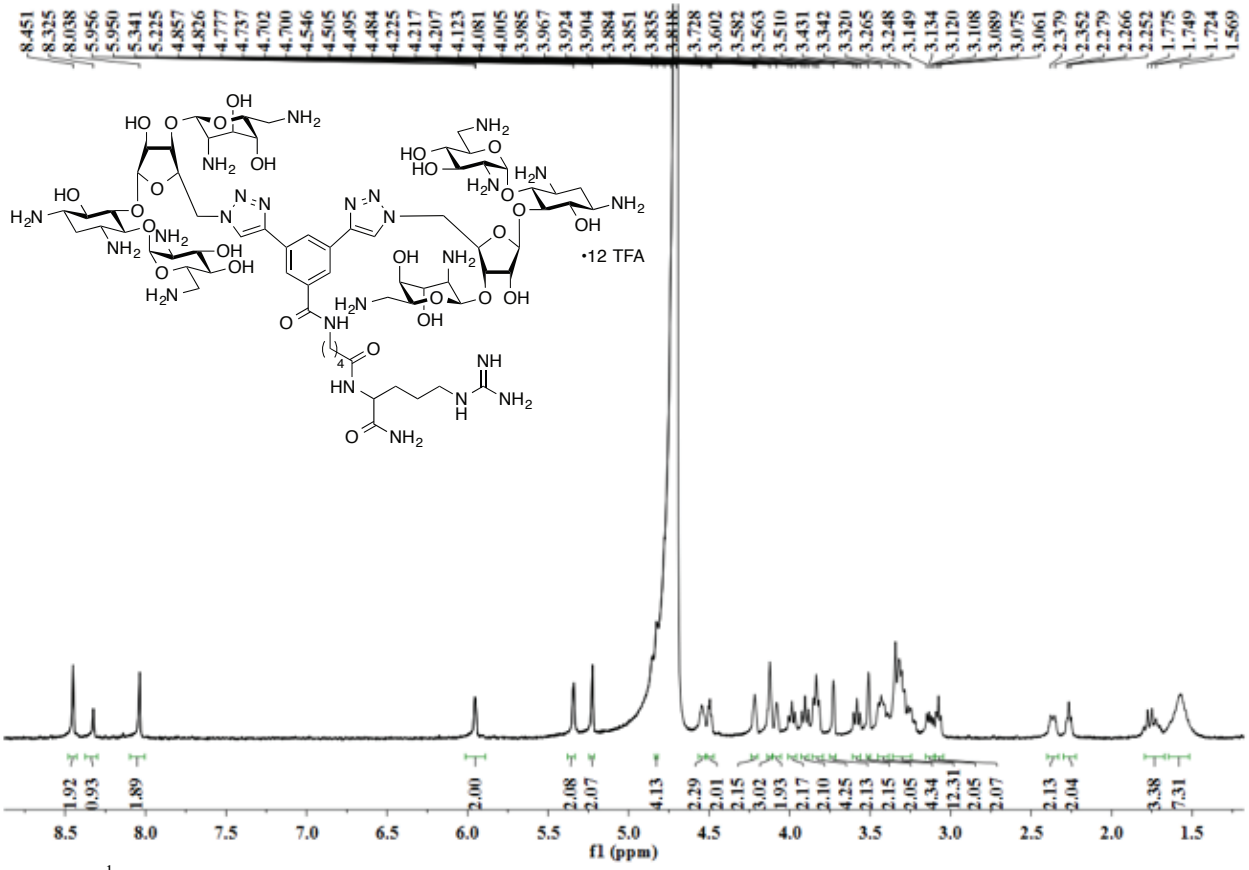

Fig. S14. ^{1}H NMR spectrum of compound **11** in D_2O.

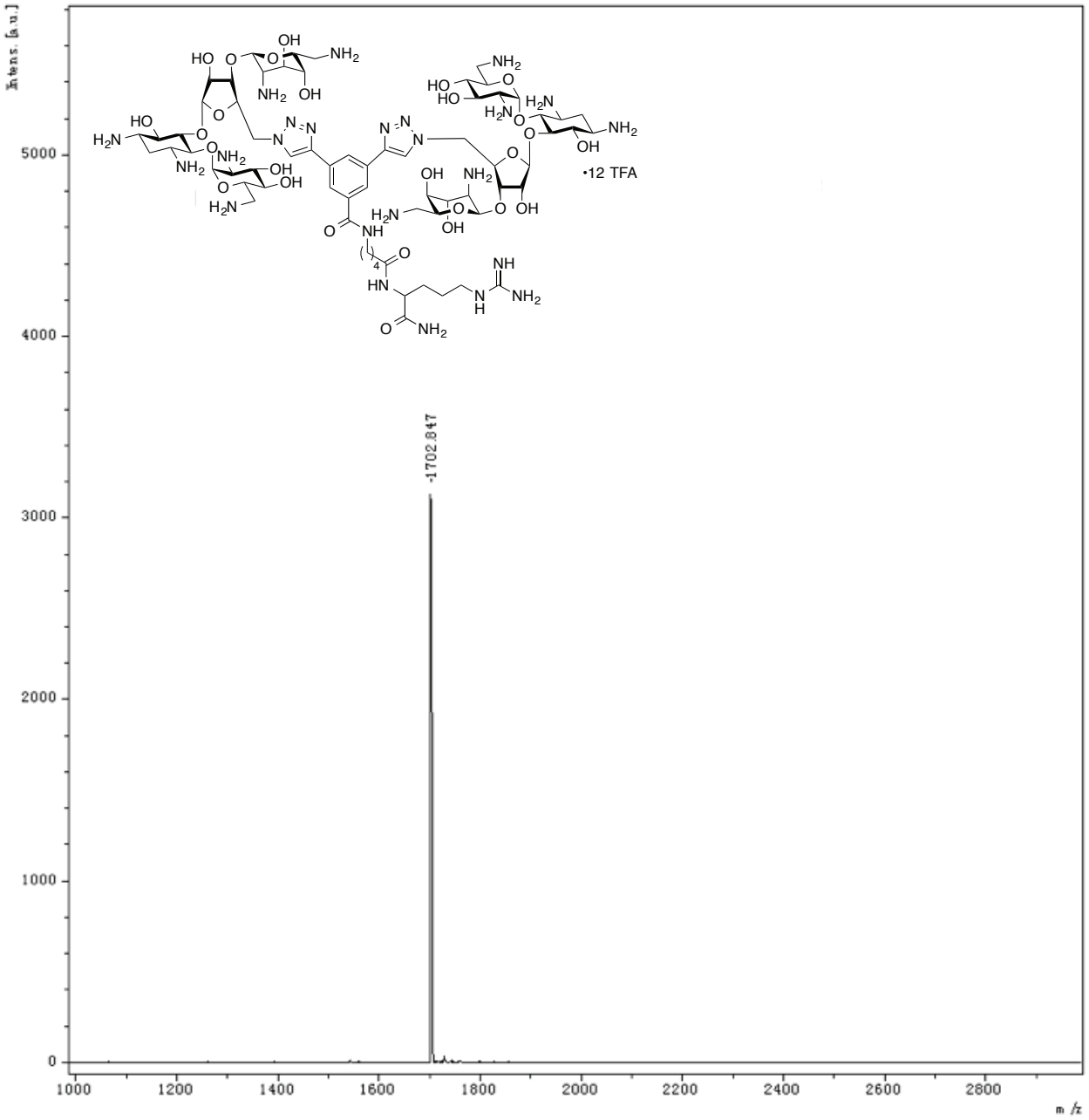

Fig. S15. MALDI-TOF MS of compound **11**.

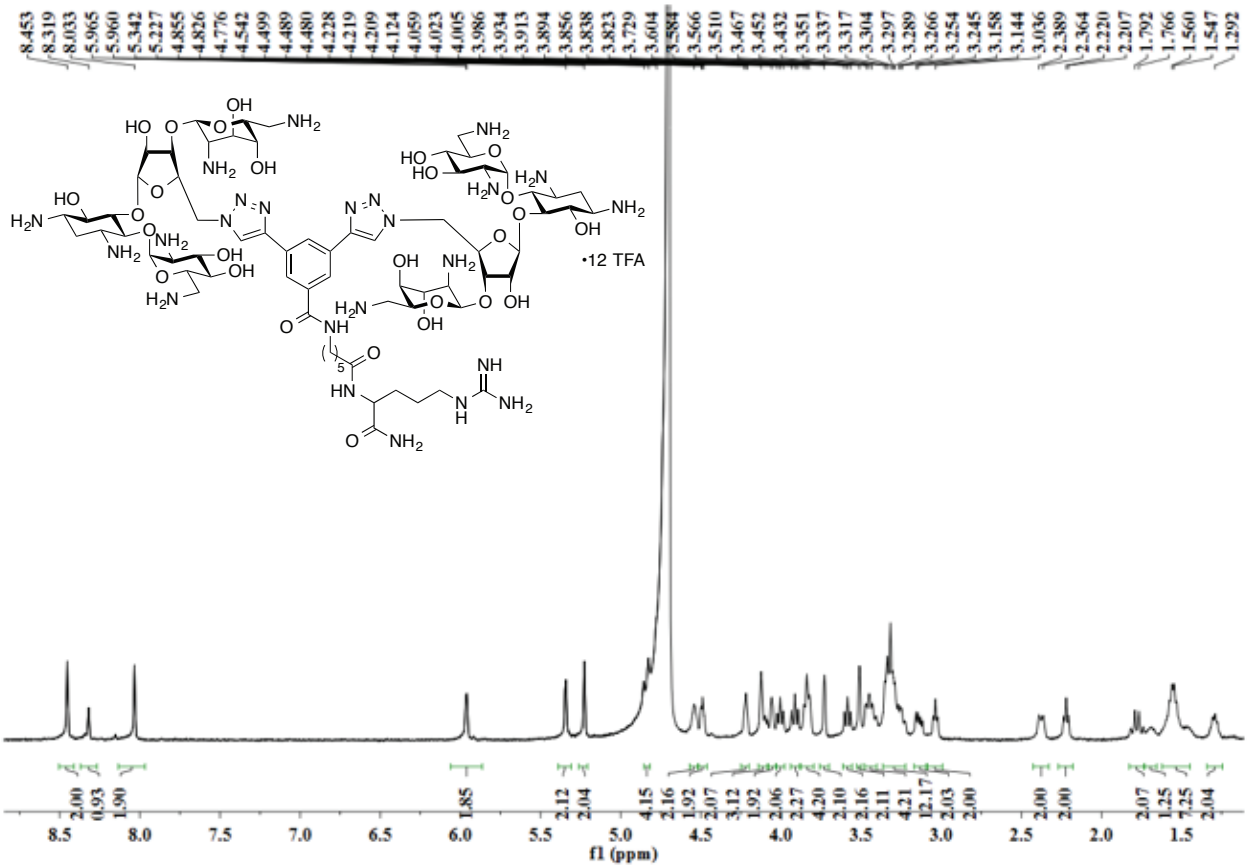

Fig. S16. ^{1}H NMR spectrum of compound **12** in D_2O.

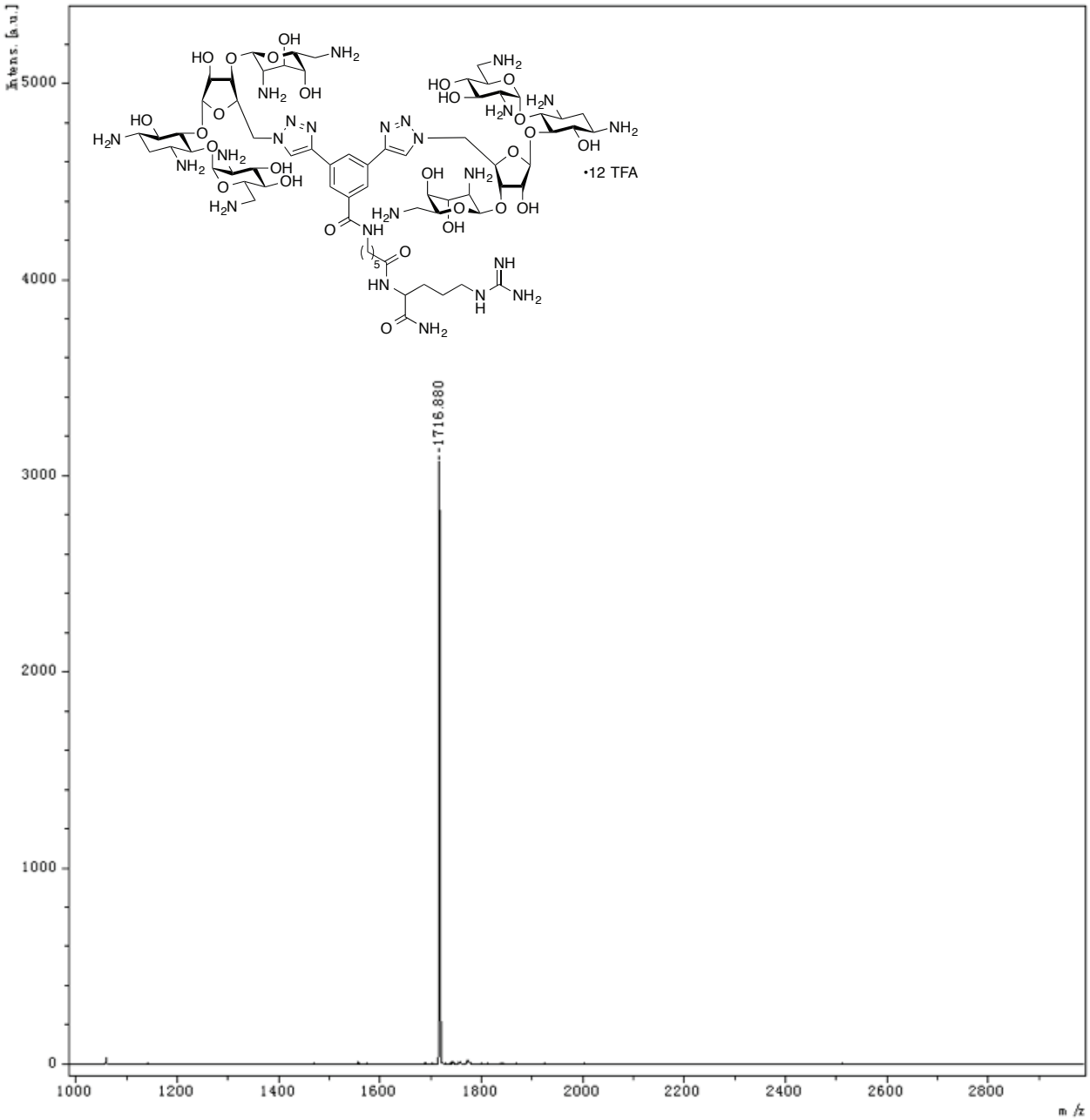

Fig. S17. MALDI-TOF MS of compound **12**.

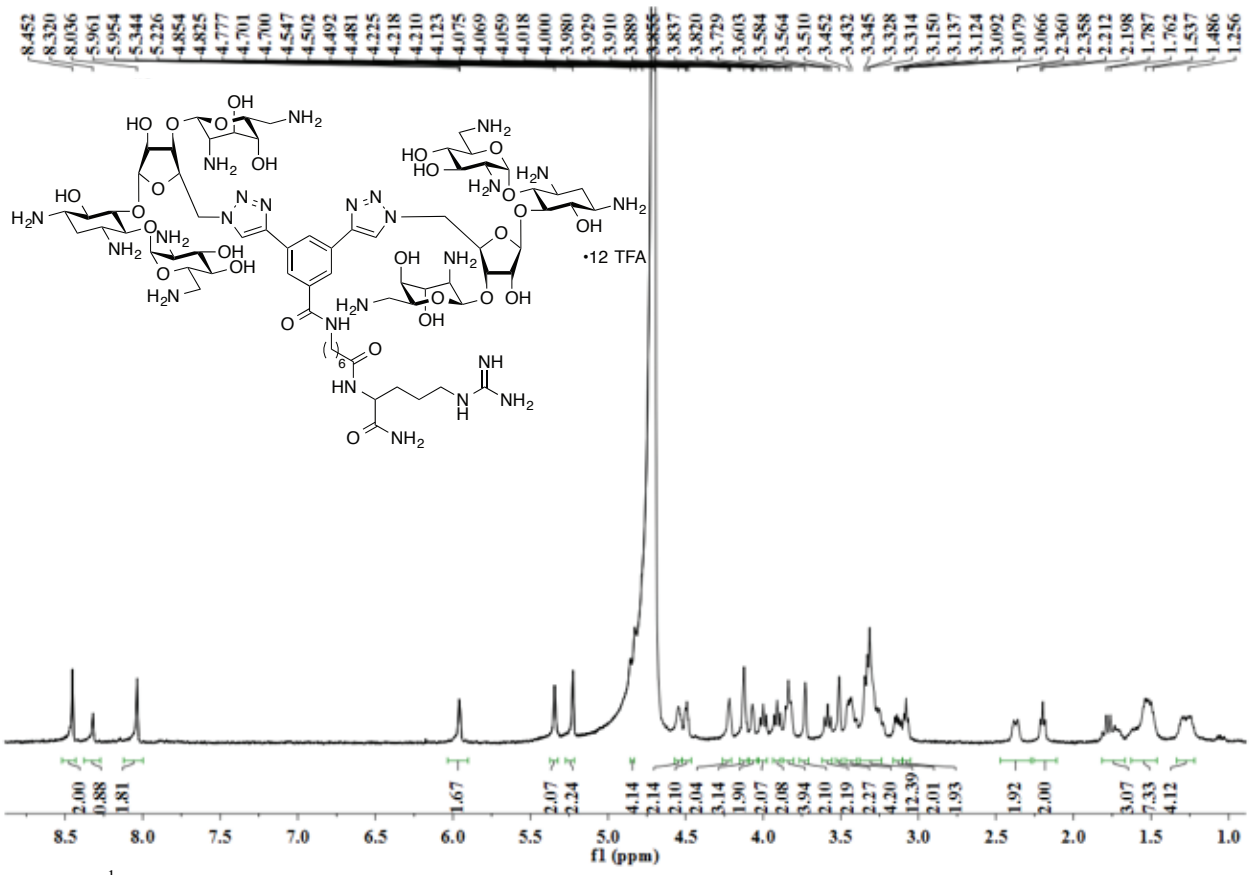

Fig. S18. ^{1}H NMR spectrum of compound **13** in D_2O.

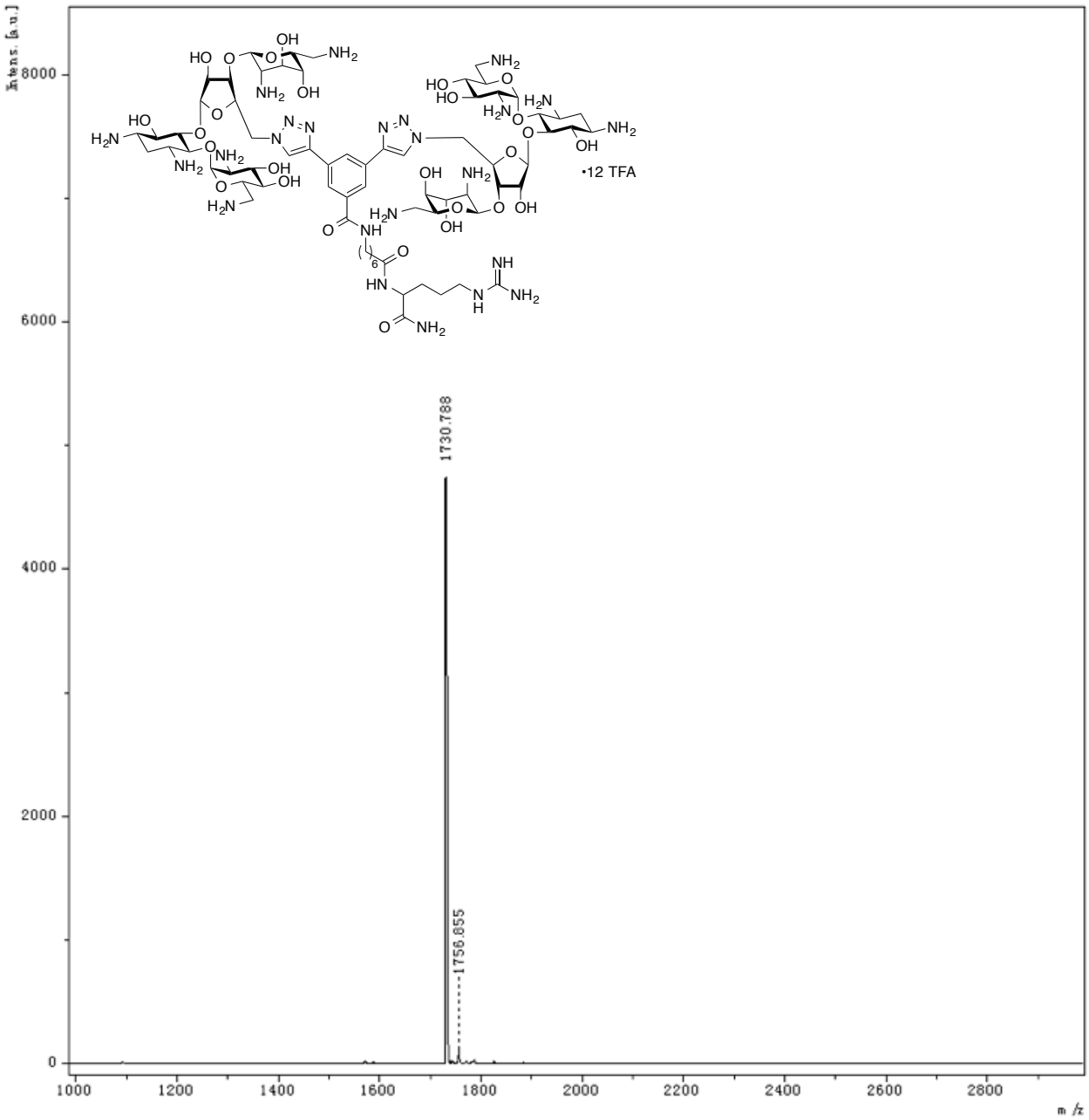

Fig. S19. MALDI-TOF MS of compound **13**.

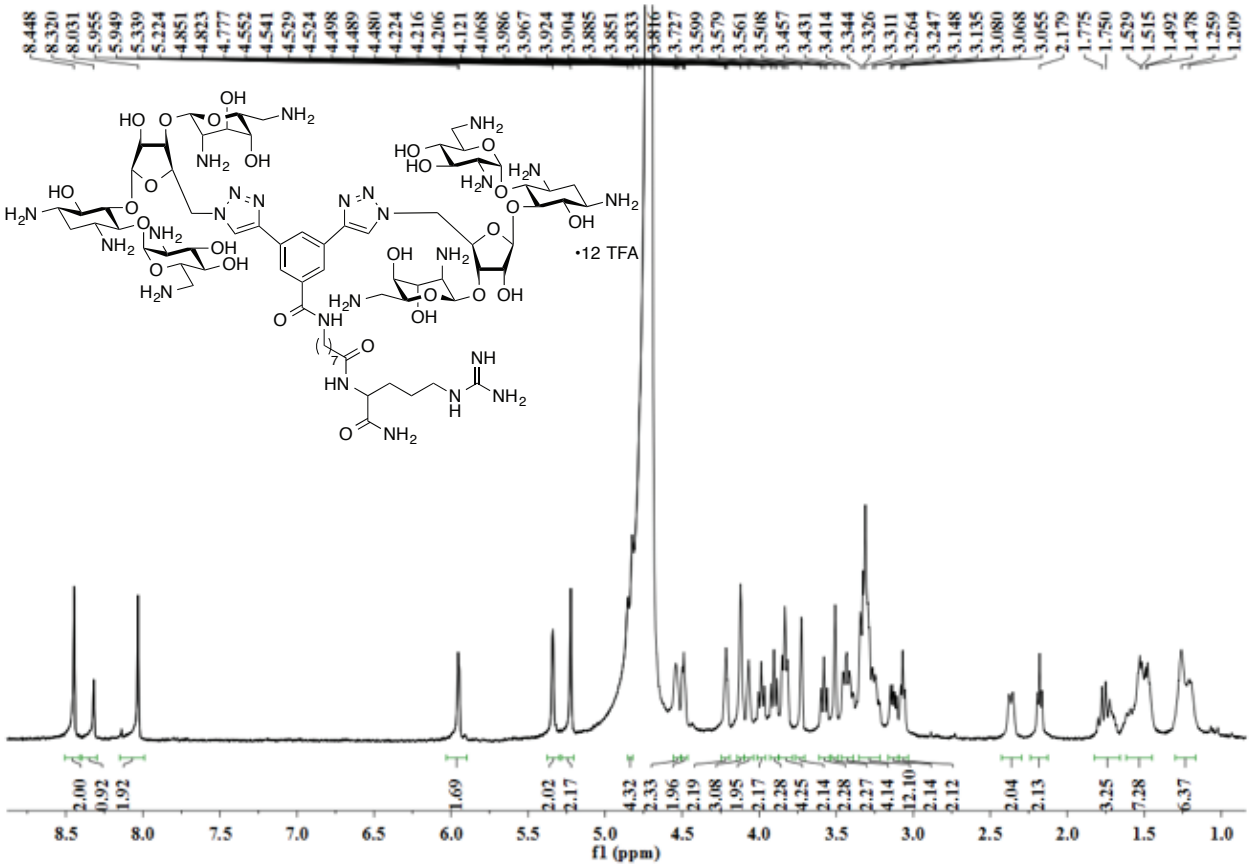

Fig. S20. ^{1}H NMR spectrum of compound **14** in D_2O.

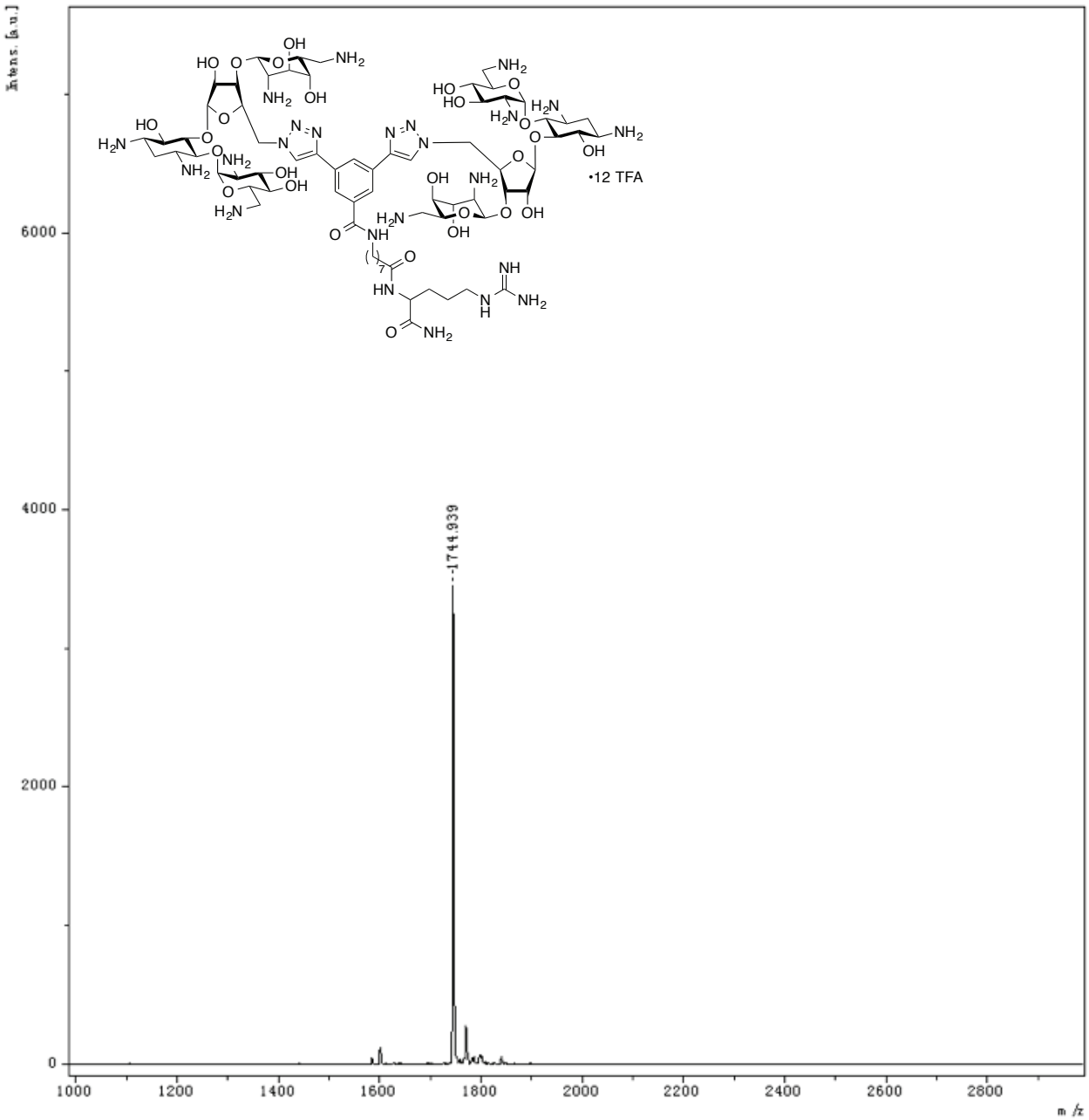

Fig. S21. MALDI-TOF MS of compound **14**.

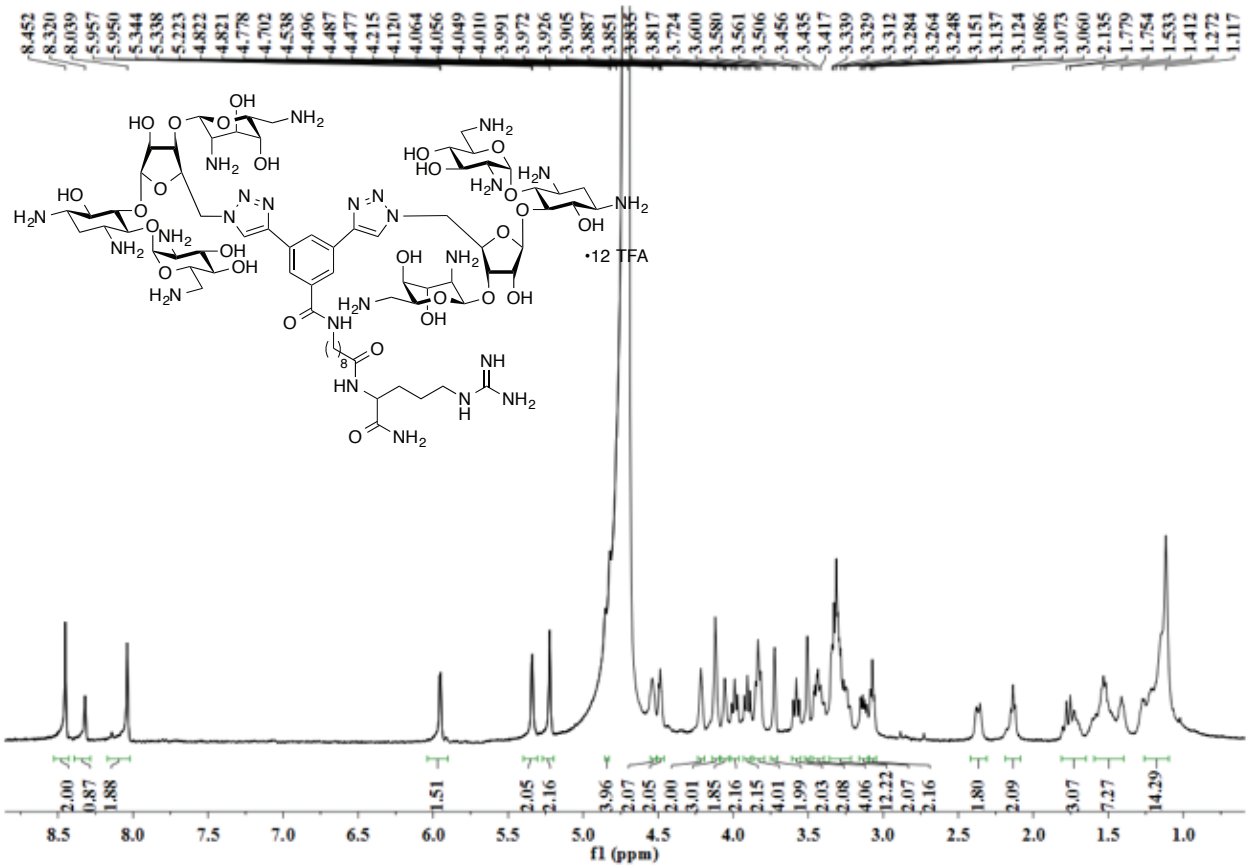

Fig. S22. ^{1}H NMR spectrum of compound **15** in D_2O.

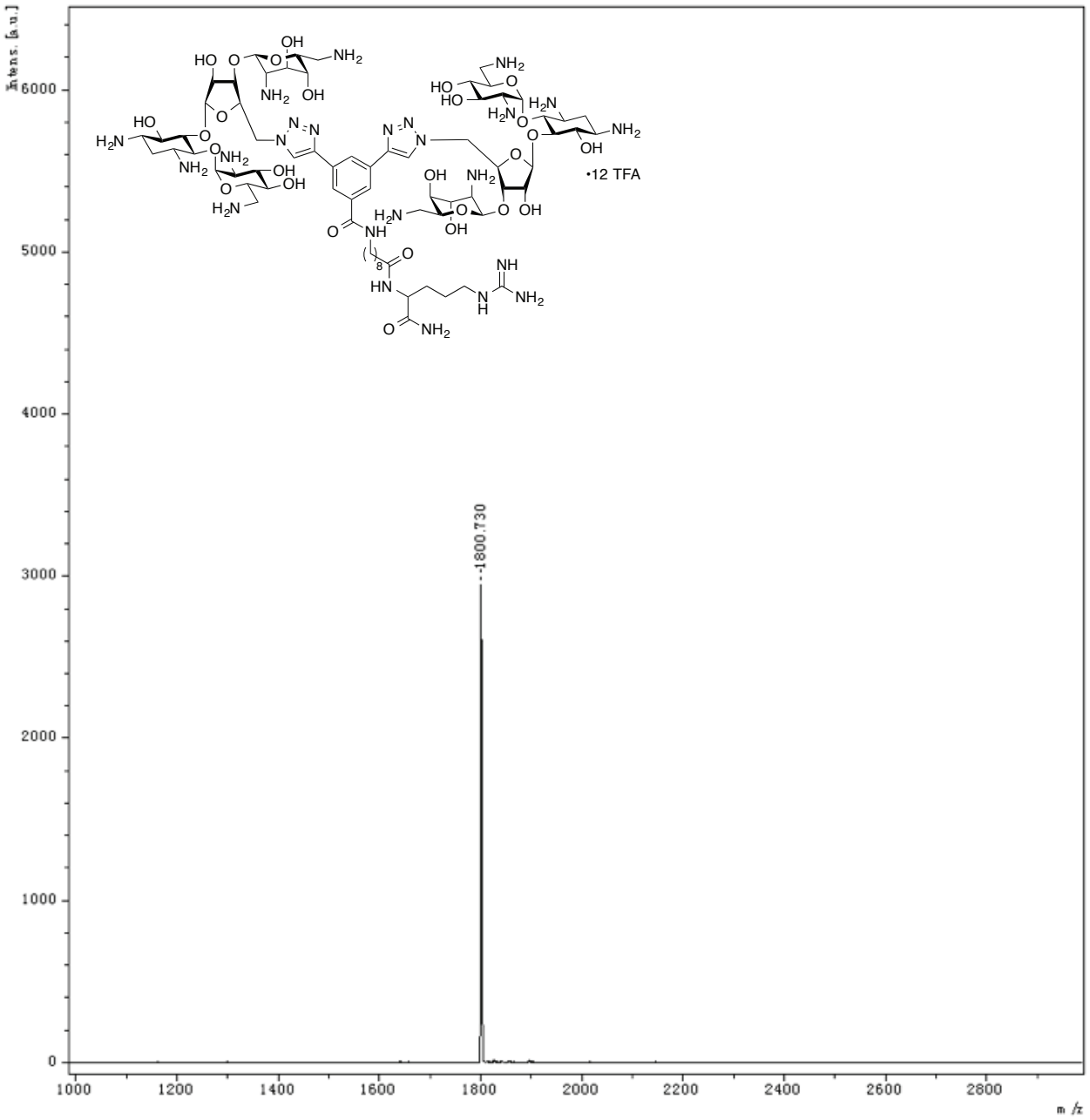

Fig. S23. MALDI-TOF MS of compound **15**.

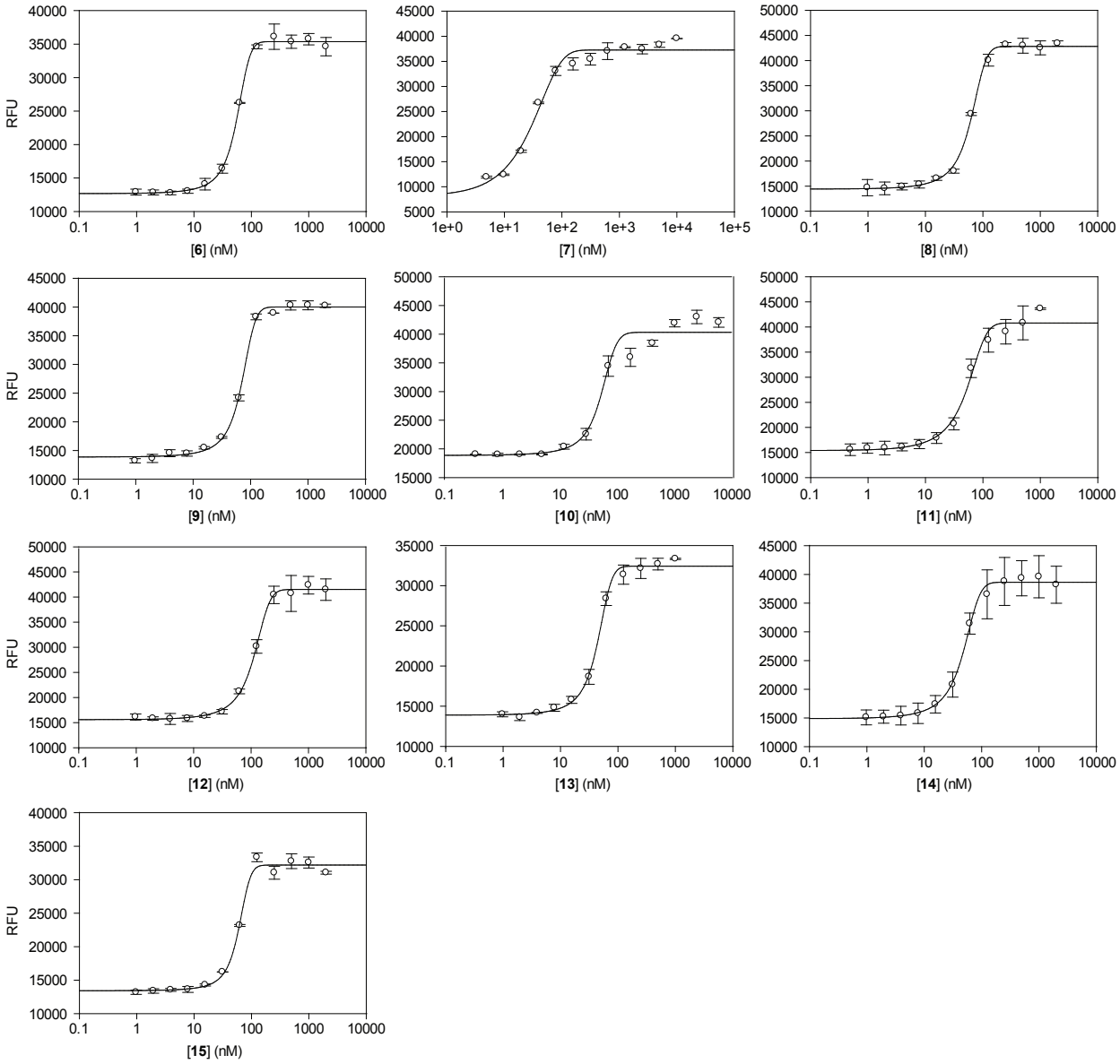

Fig. S24. Graphs for the determination of IC_{50} values for compounds **6-15** against the *E. coli* A-site.

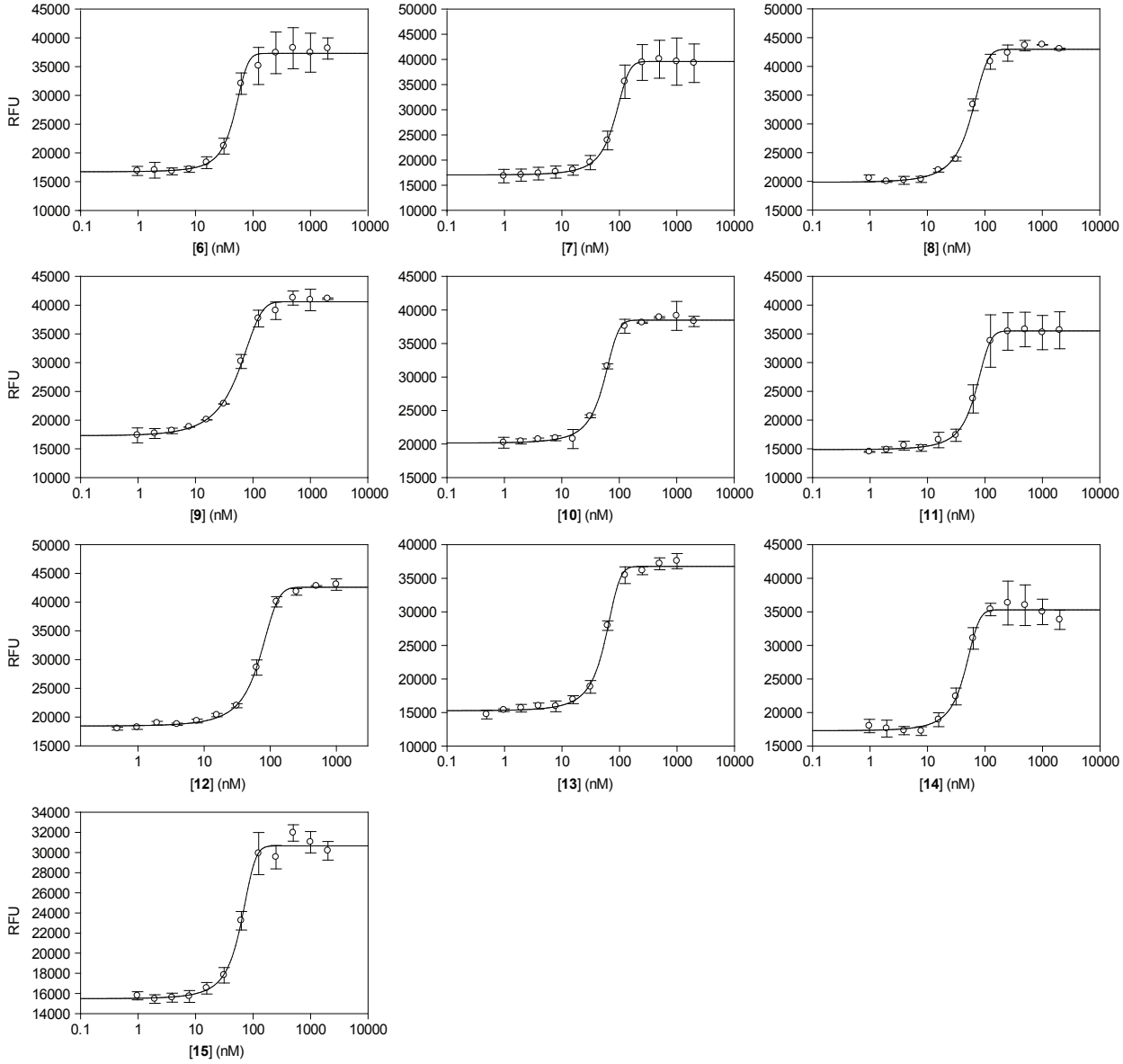

Fig. S25. Graphs for the determination of IC_{50} values for compounds **6-15** against the human A-site.